predisposing factor for the occurrence of UPD(14)pat,[11–16] such a possible chromosomal effect has been excluded in nearly all patients examined in this study.

The relative frequency of underlying causes has also been reported in other imprinting disorders.[8,17–19] The data are summarized in Table 2 (a similar summary has also been reported recently by Hoffmann *et al*).[10] In particular, the results in patients with normal karyotype are available in Prader–Willi syndrome (PWS).[8] Furthermore, PWS is also known to be caused by UPD, microdeletions, and epimutations affecting a single imprinting region,[8,19] although Silver–Russell syndrome and Beckwith–Wiedemann syndrome (BWS) can result from perturbation of at least two imprinted regions,[17,18] and BWS and Angelman syndrome can occur as a single gene disorder.[17,19] Thus, it is notable that the relative frequency of underlying causes is quite different between patients with UPD(14)pat-like phenotype and those with PWS.[8,19] This would primarily be due to the presence of low copy repeats flanking the imprinted region on chromosome 15, because chromosomal deletions are prone to occur in regions harboring such repeat sequences.[20] Indeed, two types of microdeletions mediated by such low copy repeats account for a vast majority of microdeletions in patients with PWS,[21] whereas the microdeletions identified in patients with UPD(14)pat-like phenotype are different to each other. This would explain why microdeletions are less frequent and UPD and epimutations are more frequent in patients with UPD(14)pat-like phenotype than in those with PWS.

Advanced maternal age at childbirth was predominantly observed in the MR/PE subtype. This may imply the relevance of advanced maternal age to the development of MR-mediated UPD(14)pat, because the generation of nullisomic oocytes through M1 non-disjunction is a maternal age-dependent phenomenon.[22] Although no paternal age effect was observed, this is consistent with the previous data indicating no association of advanced paternal age with a meiotic error.[23] For the maternal age effect, however, several matters should be pointed out: (1) the number of analyzed patients is small, although it is very difficult to collect a large number of patients in this extremely rare disorder; (2) of the MR/PE subtype, the advanced maternal age is a risk factor for the generation of MR-mediated UPD(14)pat, but not for the development of PE-mediated UPD(14)pat; (3) it is impossible to discriminate between maternal age-dependent M1 non-disjunction and maternal age-independent M2 non-disjunction in the MR and GC subtypes (however, GC must be extremely rare, because it requires the concomitant occurrence of a nullisomic oocyte and a disomic sperm); (4) of the TR/GC subtype, the advanced maternal age is a risk factor for the generation of GC-mediated UPD(14)pat, but not for the development of TR-mediated UPD(14)pat; and (5) if a cryptic recombination(s) might remain undetected in some patients with apparently full isodisomy, this argues that such patients actually have TR- or GC-mediated UPD(14)pat rather than MR- or PE-mediated UPD(14)pat. Thus, further studies are required to examine the maternal age effect on the generation of MR-mediated UPD(14)pat. In addition, while a relationship is unlikely to exist between advanced maternal age and microdeletions and epimutations, this notion would also await further investigations.

Such a maternal age effect is also expected in the TR/GC subtype maternal UPDs after M1 non-disjunction, because the generation of disomic oocytes through M1 non-disjunction is also a maternal age-dependent phenomenon.[7] Indeed, such a maternal age effect has been shown for PWS patients with normal karyotype; the maternal age at childbirth was significantly higher in patients with heterodisomy for a very pericentromeric region indicative of TR/GC subtype UPD(15)mat after M1 non-disjunction than in those with other genetic causes.[8,9] For various chromosomes other than chromosome 15, furthermore, since maternal age at childbirth is higher in patients with maternal heterodisomy than in those with maternal isodisomy,[24] this would also argue for maternal age effect on the development of maternal UPDs. However, in the previous studies on maternal UPDs other than UPD(15)mat, the available data are quite insufficient to assess the maternal age effect. For example, although a relatively large number of patients with UPD(14)mat phenotype have been reported in the literature (reviewed in reference Hoffmann *et al*),[10] we could identify only six UPD(14)mat patients with normal karyotype in whom maternal age at childbirth was documented and microsatellite analysis was performed.[25–30] Furthermore, the microsatellite data are insufficient to identify the subtype of UPD(14)mat and to distinguish between M1 and M2 non-disjunction in the TR/GC subtype. Thus, while the maternal age at childbirth may be advanced in five patients with apparently TR/GC-mediated UPD(14)mat (27, 35, 37, 41, and 44 years)[25–27,29,30] (the maternal age at childbirth in the remaining one

Table 2 Relative frequency of genetic mechanisms in imprinting disorders

	UPD(14)pat-like phenotype	*BWS*	*SRS*	*AS*	*PWS*
Uniparental disomy	65.4%	16%	10%	3–5%	25% (25%)
	UPD(14)pat	UPD(11)pat (mosaic)	UPD(7)mat	UPD(15)pat	UPD(15)mat
Cryptic deletion	19.2%	Rare	—	70%	70% (72%)
Cryptic duplication	—	—	Rare	—	—
Epimutation					
Hypermethylation	15.4%	9%	—	—	2–5% (2%)
Affected DMR	IG-DMR/*MEG3*-DMR	*H19*-DMR	—	—	*SNRPN*-DMR
Hypomethylation	—	44%	>38%	2–5%	—
Affected DMR		KvDMR1	*H19*-DMR	*SNRPN*-DMR	
Gene mutation	—	5%	—	10-15%	—
Mutated gene		*CDKN1C*		*UBE3A*	
Unknown		25%	>40%	10%	
Reference	This study	15	16	17	8, 17

Abbreviations: AS, Angelman syndrome; BWS, Beckwith–Wiedemann syndrome; PWS, Prader–Willi syndrome; SRS, Silver–Russell syndrome.
Patients with abnormal karyotypes are included in BWS and AS, and not included in SRS. In PWS, the data including patients with abnormal karyotypes are shown, and those from patients with normal karyotype alone are depicted in parentheses.

patient with apparently MR/PE-mediated UPD(14)mat is 40 years),[28] the notion of a maternal age effect awaits further investigations for UPD(14)mat.

Finally, it appears to be worth pointing out that methylation analysis invariably revealed hypermethylated DMR(s) in all the 26 patients who were initially ascertained because of bell-shaped thorax with coat-hanger appearance of the ribs. This indicates that methylation analysis of the DMRs can be utilized for a screening of this condition, and that the constellation of clinical features in the UPD(14)pat-like phenotype, especially the bell-shaped thorax with coat-hanger appearance of the ribs, is highly unique to patients with UPD(14)pat-like phenotype.

In summary, this study confirms the relative frequency of underlying genetic causes for the UPD(14)pat phenotype and reveals the relative frequency of UPD(14)pat subtypes. Furthermore, the results emphasize the difference in the relative frequency of underlying genetic causes among imprinted disorders, and may support a possible maternal age effect on the generation of the nullisomic oocyte mediated UPD(14)pat. Further studies will permit a more precise assessment on these matters.

CONFLICT OF INTEREST

The authors declare no conflict of interest.

ACKNOWLEDGEMENTS

We thank Drs Kenji Kurosawa, Michiko Hayashidani, Toshio Takeuchi, Shinya Tanaka, Mika Noguch, Kouji Masumoto, Takeshi Utsunomiya, Yumiko Komatsu, Hirofumi Ohashi, Maureen J O'Sullivan, Andrew J Green, Yoshiyuki Watabe, Tsuyako Iwai, Hitoshi Kawato, Miho Torikai, Akiko Yamamoto, Nobuhiro Suzumori, Makoto Kuwajima, Hiroshi Yoshihashi, Yoriko Watanabe, and Jin Nishimura for material sampling and phenotype assessment. This work was supported by Grants for Research on Intractable Diseases (H22-161) and for Health Research on Children, Youth and Families (H21-005) from the Ministry of Health, Labor and Welfare, by Grants-in-Aid for Scientific Research (A) (22249010) and (B) (21028026) from the Japan Society for the Promotion of Science (JSPS), by Grants from Takeda Science Foundation and from Kanehara Foundation, and by the Grant for National Center for Child Health and Development (23A-1).

1 da Rocha ST, Edwards CA, Ito M, Ogata T, Ferguson-Smith AC: Genomic imprinting at the mammalian Dlk1-Dio3 domain. *Trends Genet* 2008; **24**: 306–316.
2 Kagami M, Sekita Y, Nishimura G *et al*: Deletions and epimutations affecting the human 14q32.2 imprinted region in individuals with paternal and maternal upd(14)-like phenotypes. *Nat Genet* 2008; **40**: 237–242.
3 Kagami M, O'Sullivan MJ, Green AJ *et al*: The IG-DMR and the MEG3-DMR at human chromosome 14q32.2: hierarchical interaction and distinct functional properties as imprinting control centers. *PLoS Genet* 2010; **6**: e1000992.
4 Kagami M, Nishimura G, Okuyama T *et al*: Segmental and full paternal isodisomy for chromosome 14 in three patients: narrowing the critical region and implication for the clinical features. *Am J Med Genet A* 2005; **138A**: 127–132.
5 Kagami M, Yamazawa K, Matsubara K, Matsuo N, Ogata T: Placentomegaly in paternal uniparental disomy for human chromosome 14. *Placenta* 2008; **29**: 760–761.
6 Shaffer LG, Agan N, Goldberg JD, Ledbetter DH, Longshore JW, Cassidy SB: American College of Medical Genetics statement of diagnostic testing for uniparental disomy. *Genet Med* 2001; **3**: 206–211.
7 Jones KT: Meiosis in oocytes: predisposition to aneuploidy and its increased incidence with age. *Hum Reprod Update* 2008; **14**: 143–158.
8 Matsubara K, Murakami N, Nagai T, Ogata T: Maternal age effect on the development of Prader-Willi syndrome resulting from upd(15)mat through meiosis 1 errors. *J Hum Genet* 2011; **56**: 566–571.
9 Robinson WP, Christian SL, Kuchinka BD *et al*: Somatic segregation errors predominantly contribute to the gain or loss of a paternal chromosome leading to uniparental disomy for chromosome 15. *Clin Genet* 2000; **57**: 349–358.
10 Hoffmann K, Heller R: Uniparental disomies 7 and 14. *Best Pract Res Clin Endocrinol Metab* 2011; **25**: 77–100.
11 Wang JC, Passage MB, Yen PH, Shapiro LJ, Mohandas TK: Uniparental heterodisomy for chromosome 14 in a phenotypically abnormal familial balanced 13/14 Robertsonian translocation carrier. *Am J Hum Genet* 1991; **48**: 1069–1074.
12 Papenhausen PR, Mueller OT, Johnson VP, Sutcliffe M, Diamond TM, Kousseff BG: Uniparental isodisomy of chromosome 14 in two cases: an abnormal child and a normal adult. *Am J Med Genet* 1995; **59**: 271–275.
13 Cotter PD, Kaffe S, McCurdy LD, Jhaveri M, Willner JP, Hirschhorn K: Paternal uniparental disomy for chromosome 14: a case report and review. *Am J Med Genet* 1997; **70**: 74–79.
14 Yano S, Li L, Owen S, Wu S, Tran T: A further delineation of the paternal uniparental disomy (UPD14): the fifth reported liveborn case. *Am J Hum Genet* 2001; **69** (Suppl): A739.
15 Kurosawa K, Sasaki H, Sato Y *et al*: Paternal UPD14 is responsible for a distinctive malformation complex. *Am J Med Genet A* 2002; **110**: 268–272.
16 McGowan KD, Weiser JJ, Horwitz J *et al*: The importance of investigating for uniparental disomy in prenatally identified balanced acrocentric rearrangements. *Prenat Diagn* 2002; **22**: 141–143.
17 Sasaki K, Soejima H, Higashimoto K *et al*: Japanese and North American/European patients with Beckwith-Wiedemann syndrome have different frequencies of some epigenetic and genetic alterations. *Eur J Hum Genet* 2007; **15**: 1205–1210.
18 Eggermann T: Epigenetic regulation of growth: lessons from Silver-Russell syndrome. *Endocr Dev* 2009; **14**: 10–19.
19 Gurrieri F, Accadia M: Genetic imprinting: the paradigm of Prader-Willi and Angelman syndromes. *Endocr Dev* 2009; **14**: 20–28.
20 Pujana MA, Nadal M, Guitart M, Armengol L, Gratacos M, Estivill X: Human chromosome 15q11-q14 regions of rearrangements contain clusters of LCR15 duplicons. *Eur J Hum Genet* 2002; **10**: 26–35.
21 Varela MC, Kok F, Setian N, Kim CA, Koiffmann CP: Impact of molecular mechanisms, including deletion size, on Prader-Willi syndrome phenotype: study of 75 patients. *Clin Genet* 2005; **67**: 47–52.
22 Pellestor F, Andreo B, Anahory T, Hamamah S: The occurrence of aneuploidy in human: lessons from the cytogenetic studies of human oocytes. *Eur J Med Genet* 2006; **49**: 103–116.
23 Sloter E, Nath J, Eskenazi B, Wyrobek AJ: Effects of male age on the frequencies of germinal and heritable chromosomal abnormalities in humans and rodents. *Fertil Steril* 2004; **81**: 925–943.
24 Kotzot D: Advanced parental age in maternal uniparental disomy (UPD): implications for the mechanism of formation. *Eur J Hum Genet* 2004; **12**: 343–346.
25 Fokstuen S, Ginsburg C, Zachmann M, Schinzel A: Maternal uniparental disomy 14 as a cause of intrauterine growth retardation and early onset of puberty. *J Pediatr* 1999; **134**: 689–695.
26 Hordijk R, Wierenga H, Scheffer H, Leegte B, Hofstra RM, Stolte-Dijkstra I: Maternal uniparental disomy for chromosome 14 in a boy with a normal karyotype. *J Med Genet* 1999; **36**: 782–785.
27 Sanlaville D, Aubry MC, Dumez Y *et al*: Maternal uniparental heterodisomy of chromosome 14: chromosomal mechanism and clinical follow up. *J Med Genet* 2000; **37**: 525–528.
28 Towner DR, Shaffer LG, Yang SP, Walgenbach DD: Confined placental mosaicism for trisomy 14 and maternal uniparental disomy in association with elevated second trimester maternal serum human chorionic gonadotrophin and third trimester fetal growth restriction. *Prenat Diagn* 2001; **21**: 395–398.
29 Aretz S, Raff R, Woelfle J *et al*: Maternal uniparental disomy 14 in a 15-year-old boy with normal karyotype and no evidence of precocious puberty. *Am J Med Genet A* 2005; **135**: 336–338.
30 Mitter D, Buiting K, von Eggeling F *et al*: Is there a higher incidence of maternal uniparental disomy 14 [upd(14)mat]? Detection of 10 new patients by methylation-specific PCR. *Am J Med Genet A* 2006; **140**: 2039–2049.

Supplementary Information accompanies the paper on European Journal of Human Genetics website (http://www.nature.com/ejhg)

Journal of Human Genetics (2011) 56, 91–93

www.nature.com/jhg

SHORT COMMUNICATION

Androgenetic/biparental mosaicism in a girl with Beckwith–Wiedemann syndrome-like and upd(14)pat-like phenotypes

Kazuki Yamazawa[1,5], Kazuhiko Nakabayashi[2], Kentaro Matsuoka[3], Keiko Masubara[1], Kenichiro Hata[2], Reiko Horikawa[4] and Tsutomu Ogata[1]

This report describes androgenetic/biparental mosaicism in a 4-year-old Japanese girl with Beckwith–Wiedemann syndrome (BWS)-like and paternal uniparental disomy 14 (upd(14)pat)-like phenotypes. We performed methylation analysis for 18 differentially methylated regions on various chromosomes, genome-wide microsatellite analysis for a total of 90 loci and expression analysis of *SNRPN* in leukocytes. Consequently, she was found to have an androgenetic 46,XX cell lineage and a normal 46,XX cell lineage, with the frequency of the androgenetic cells being roughly calculated as 91% in leukocytes, 70% in tongue tissues and 79% in tonsil tissues. It is likely that, after a normal fertilization between an ovum and a sperm, the paternally derived pronucleus alone, but not the maternally derived pronucleus, underwent a mitotic division, resulting both in the generation of the androgenetic cell lineage by endoreplication of one blastomere containing a paternally derived pronucleus and in the formation of the normal cell lineage by union of paternally and maternally derived pronuclei. It appears that the extent of overall (epi)genetic aberrations exceeded the threshold level for the development of BWS-like and upd(14)pat-like phenotypes, but not for the occurrence of other imprinting disorders or recessive Mendelian disorders.
Journal of Human Genetics (2011) **56,** 91–93; doi:10.1038/jhg.2010.142; published online 11 November 2010

Keywords: androgenesis; Beckwith–Wiedemann syndrome; mosaicism; upd(14)pat

INTRODUCTION

A pure androgenetic human with paternal uniparental disomy for all chromosomes is incompatible with life because of genomic imprinting.[1,2] However, a human with an androgenetic cell lineage could be viable in the presence of a normal cell lineage. Indeed, an androgenetic cell lineage has been identified in six liveborn individuals with variable phenotypes.[3–7] All the androgenetic cell lineages have a 46,XX karyotype, and this is consistent with the lethality of an androgenetic 46,YY cell lineage.

Here, we report on a girl with androgenetic/biparental mosaicism, and discuss the underlying factors for the phenotypic development.

CASE REPORT

This patient was conceived naturally to non-consanguineous and healthy parents. At 24 weeks gestation, the mother was referred to us because of threatened premature delivery. Ultrasound studies showed Beckwith–Wiedemann syndrome (BWS)-like features,[8] such as macroglossia, organomegaly and umbilical hernia, together with polyhydramnios and placentomegaly. The mother repeatedly received amnioreduction and tocolysis.

She was delivered by an emergency cesarean section because of preterm rupture of membranes at 34 weeks of gestation. Her birth weight was 3730 g (+4.8 s.d. for gestational age), and her length 45.6 cm (+0.7 s.d.). The placenta weighed 1040 g (+7.3 s.d.).[9] She was admitted to a neonatal intensive care unit due to asphyxia. Physical examination confirmed a BWS-like phenotype. Notably, chest roentgenograms delineated mild bell-shaped thorax characteristic of paternal uniparental disomy 14 (upd(14)pat),[10] although coat hanger appearance of the ribs indicative of upd(14)pat was absent (Supplementary Figure 1). She was placed on mechanical ventilation for 2 months, and received tracheostomy, glossectomy and tonsillectomy in her infancy, due to upper airway obstruction. She also had several clinical features occasionally reported in BWS[8] (Supplementary Table 1). Her karyotype was 46,XX in all the 50 lymphocytes analyzed. On the last examination at 4 years of age, she showed postnatal growth failure and severe developmental retardation.

[1]Department of Molecular Endocrinology, National Research Institute for Child Health and Development, Tokyo, Japan; [2]Department of Maternal-Fetal Biology, National Research Institute for Child Health and Development, Tokyo, Japan; [3]Division of Pathology, National Medical Center for Children and Mothers, Tokyo, Japan and [4]Division of Endocrinology and Metabolism, National Medical Center for Children and Mothers, Tokyo, Japan
[5]Current address: Department of Physiology, Development & Neuroscience, University of Cambridge, Cambridge, UK.
Correspondence: Dr T Ogata, Department of Molecular Endocrinology, National Research Institute for Child Health and Development, 2-10-1 Ohkura, Setagaya, Tokyo 157-8535, Japan.
E-mail: tomogata@nch.go.jp
Received 9 September 2010; revised 18 October 2010; accepted 22 October 2010; published online 11 November 2010

MOLECULAR STUDIES

This study was approved by the Institutional Review Board Committee at the National Center for Child health and Development, and performed after obtaining informed consent.

Methylation analysis

We first performed bisulfite sequencing for the *H19*-DMR (differentially methylated region) and KvDMR1 as a screening of BWS[11,12] and that for the IG-DMR and the *MEG3*-DMR as a screening of upd(14)pat,[10] using leukocyte genomic DNA. Paternally derived clones were predominantly identified for the four DMRs examined (Figure 1a). We next performed combined bisulfite restriction analysis for multiple DMRs, as reported previously.[13] All the autosomal DMRs exhibited markedly skewed methylation patterns consistent with predominance of paternally inherited clones, whereas the *XIST*-DMR on the X chromosome showed a normal methylation pattern (Figure 1a).

Genome-wide microsatellite analysis

Microsatellite analysis was performed for 90 loci with high heterozygosities in the Japanese population.[14] Major peaks consistent with paternal uniparental isodisomy and minor peaks of maternal origin were identified for at least one locus on each chromosome, with the minor peaks of maternal origin being more obvious in tongue and tonsil tissues than in leukocytes (Figure 1b and Supplementary Table 2). There were no loci with three or four peaks indicative of chimerism. The frequency of the androgenetic cells was calculated as 91% in leukocytes, 70% in tongue cells and 79% in tonsil cells, although the estimation apparently was a rough one (for details, see Supplementary Methods).

Expression analysis

We examined *SNRPN* expression, because *SNRPN* showed strong expression in leukocytes (for details, see Supplementary Data). *SNRPN* expression was almost doubled in the leukocytes of this patient (Figure 1c).

DISCUSSION

These results suggest that this patient had an androgenetic 46,XX cell lineage and a normal 46,XX cell lineage. In this regard, both the androgenetic and the biparental cell lineages appear to have derived from a single sperm and a single ovum, because a single haploid genome of paternal origin and that of maternal origin were identified in this patient by genome-wide microsatellite analysis. Thus, it is likely that after a normal fertilization between an ovum and a sperm, the paternally derived pronucleus alone, but not the maternally derived pronucleus, underwent a mitotic division, resulting both in the generation of the androgenetic cell lineage by endoreplication of

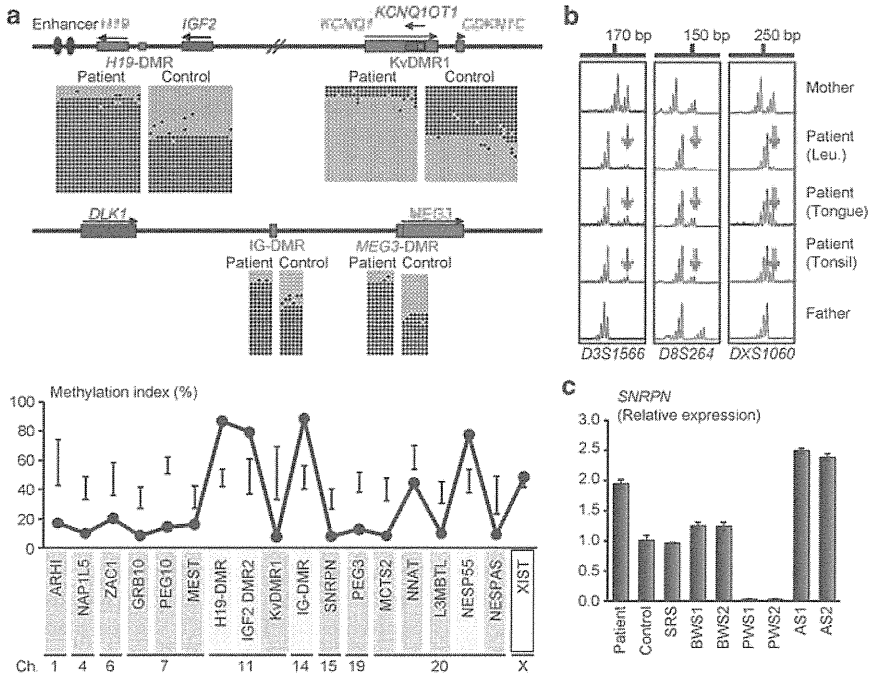

Figure 1 Representative molecular results. (**a**) Methylation analysis. Upper part: Bisulfite sequencing data for the *H19*-DMR and the KvDMR1 on 11p15.5, and those for the IG-DMR and the *MEG3*-DMR on 14q32.2. Each line indicates a single clone, and each circle denotes a CpG dinucleotide; filled and open circles represent methylated and unmethylated cytosines, respectively. Paternally expressed genes are shown in blue, maternally expressed gene in red, and the DMRs in green. The *H19*-DMR, the IG-DMR, and the *MEG3*-DMR are usually methylated after paternal transmission and unmethylated after maternal transmission, whereas the KvDMR1 is usually unmethylated after paternal transmission and methylated after maternal transmission.[10,11] Lower part: Methylation indices (the ratios of methylated clones) obtained from the COBRA analyses for the 18 DMRs. The DMRs highlighted in blue and pink are methylated after paternal and maternal transmissions, respectively. The black vertical bars indicate the reference data (maximum – minimum) in leukocyte genomic DNA of 20 normal control subjects (the *XIST*-DMR data are obtained from 16 control females). (**b**) Representative microsatellite analysis. Major peaks of paternal origin and minor peaks of maternal origin (red arrows) have been identified in this patient. The minor peaks of maternal origin are more obvious in tongue and tonsil tissues than in leukocytes (Leu.). (**c**) Relative expression level (mean ± s.d.) of *SNRPN*. The data are normalized against *TBP*. SRS: an SRS patient with an epimutation (hypomethylation) of the *H19*-DMR; BWS1: a BWS patient with an epimutation (hypermethylation) of the *H19*-DMR; BWS2: a BWS patient with upd(11)pat; PWS1: a Prader-Willi syndrome (PWS) patient with upd(15)mat; PWS2: a PWS patient with an epimutation (hypermethylation) of the *SNRPN*-DMR; AS1: an Angelman syndrome (AS) patient with upd(15)pat; and AS2: an AS patient with an epimutation (hypomethylation) of the *SNRPN*-DMR. The data were obtained using an ABI Prism 7000 Sequence Detection System (Applied Biosystems).

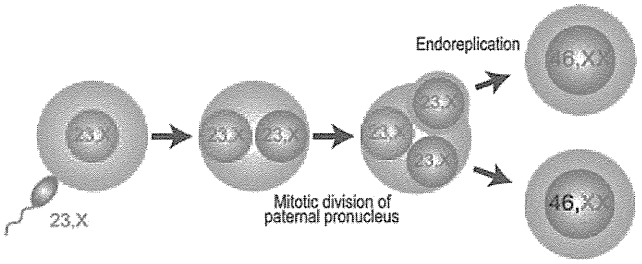

Figure 2 Schematic representation of the generation of the androgenetic/biparental mosaicism. Polar bodies are not shown.

one blastomere containing a paternally derived pronucleus and in the formation of the normal cell lineage by union of paternally and maternally derived pronuclei (Figure 2). This model has been proposed for androgenetic/biparental mosaicism generated after fertilization between a single ovum and a single sperm.[5,15,16] The normal methylation pattern of the *XIST*-DMR is explained by assuming that the two X chromosomes in the androgenetic cell lineage undergo random X-inactivation, as in the normal cell lineage. Furthermore, the results of microsatellite analysis imply that the androgenetic cells were more prevalent in leukocytes than in tongue and tonsil tissues.

A somatic androgenetic cell lineage has been identified in seven liveborn patients including this patient (Supplementary Table 1).[3–7] In this context, leukocytes are preferentially utilized for genetic analyses in human patients, and detailed examinations such as analyses of plural DMRs are necessary to detect an androgenetic cell lineage. Thus, the hitherto identified patients would be limited to those who had androgenetic cells as a predominant cell lineage in leukocytes probably because of a stochastic event and received detailed molecular studies. If so, an androgenetic cell lineage may not be so rare, and could be revealed by detailed analyses as well as examinations of additional tissues in patients with relatively complex phenotypes, as observed in the present patient.

Phenotypic features in androgenetic/biparental mosaicism would be determined by several factors. They include (1) the ratio of two cell lineages in various tissues/organs, (2) the number of imprinted domains relevant to specific features (for example, dysregulation of the imprinted domains on 11p15.5 and 14q32.2 is involved in placentomegaly[9,17]), (3) the degree of clinical effects of dysregulated imprinted domains (an (epi)dominant effect has been assumed for the 11p15.5 imprinted domains[18]), (4) expression levels of imprinted genes in androgenetic cells (although *SNRPN* expression of this patient was consistent with androgenetic cells being predominant in leukocytes, complicated expression patterns have been identified for several imprinted genes in both androgenetic and parthenogenetic fetal mice, probably because of perturbed *cis*- and *trans*-acting regulatory mechanisms[19]) and (5) unmasking of possible paternally inherited recessive mutation(s) in androgenetic cells. Thus, in this patient, it appears that the extent of overall (epi)genetic aberrations exceeded the threshold level for the development of BWS-like and upd(14)pat-like body and placental phenotypes, but remained below the threshold level for the occurrence of other imprinting disorders or recessive Mendelian disorders.

CONFLICT OF INTEREST

The authors declare no conflict of interest.

ACKNOWLEDGEMENTS

This work was supported by grants from the Ministry of Health, Labor, and Welfare, and the Ministry of Education, Science, Sports and Culture.

1 Surani, M. A., Barton, S. C. & Norris, M. L. Development of reconstituted mouse eggs suggests imprinting of the genome during gametogenesis. *Nature* **308,** 548–550 (1984).
2 McGrath, J. & Solter, D. Completion of mouse embryogenesis requires both the maternal and paternal genomes. *Cell* **37,** 179–183 (1984).
3 Hoban, P. R., Heighway, J., White, G. R., Baker, B., Gardner, J., Birch, J. M. *et al.* Genome-wide loss of maternal alleles in a nephrogenic rest and Wilms' tumour from a BWS patient. *Hum. Genet.* **95,** 651–656 (1995).
4 Bryke, C. R., Garber, A. T. & Israel, J. Evolution of a complex phenotype in a unique patient with a paternal uniparental disomy for every chromosome cell line and a normal biparental inheritance cell line. *Am. J. Hum. Genet.* **75**(Suppl), 831 (2004).
5 Giurgea, I., Sanlaville, D., Fournet, J. C., Sempoux, C., Bellanne-Chantelot, C. & Touati, G. Congenital hyperinsulinism and mosaic abnormalities of the ploidy. *J. Med. Genet.* **43,** 248–254 (2006).
6 Wilson, M., Peters, G., Bennetts, B., McGillivray, G., Wu, Z. H., Poon, C. *et al.* The clinical phenotype of mosaicism for genome-wide paternal uniparental disomy: two new reports. *Am. J. Med. Genet. Part A* **146A,** 137–148 (2008).
7 Reed, R. C., Beischel, L., Schoof, J., Johnson, J., Raff, M. L. & Kapur, R. P. Androgenetic/biparental mosaicism in an infant with hepatic mesenchymal hamartoma and placental mesenchymal dysplasia. *Pediatr. Dev. Pathol.* **11,** 377–383 (2008).
8 Jones, K. L. *Smith's Recognizable Patterns of Human Malformation* 6th edn. (Elsevier Saunders: Philadelphia, 2006).
9 Kagami, M., Yamazawa, K., Matsubara, K., Matsuo, N. & Ogata, T. Placentomegaly in paternal uniparental disomy for human chromosome 14. *Placenta* **29,** 760–761 (2008).
10 Kagami, M., Sekita, Y., Nishimura, G., Irie, M., Kato, F., Okada, M. *et al.* Deletions and epimutations affecting the human 14q32.2 imprinted region in individuals with paternal and maternal upd(14)-like phenotypes. *Nat. Genet.* **40,** 237–242 (2008).
11 Yamazawa, K., Kagami, M., Nagai, T., Kondoh, T., Onigata, K., Maeyama, K. *et al.* Molecular and clinical findings and their correlations in Silver-Russell syndrome: implications for a positive role of IGF2 in growth determination and differential imprinting regulation of the IGF2-H19 domain in bodies and placentas. *J. Mol. Med.* **86,** 1171–1181 (2008).
12 Weksberg, R., Shuman, C. & Beckwith, J. B. Beckwith-Wiedemann syndrome. *Eur. J. Hum. Genet.* **18,** 8–14 (2010).
13 Yamazawa, K., Nakabayashi, K., Kagami, M., Sato, T., Saitoh, S., Horikawa, R. *et al.* Parthenogenetic chimaerism/mosaicism with a Silver-Russell syndrome-like phenotype. *J. Med. Genet.* **47,** 782–785 (2010).
14 Ikari, K., Onda, H., Furushima, K., Maeda, S., Harata, S. & Takeda, J. Establishment of an optimized set of 406 microsatellite markers covering the whole genome for the Japanese population. *J. Hum. Genet.* **46,** 207–210 (2001).
15 Kaiser-Rogers, K. A., McFadden, D. E., Livasy, C. A., Dansereau, J., Jiang, R., Knops, J. F. *et al.* Androgenetic/biparental mosaicism causes placental mesenchymal dysplasia. *J. Med. Genet.* **43,** 187–192 (2006).
16 Kotzot, D. Complex and segmental uniparental disomy updated. *J. Med. Genet.* **45,** 545–556 (2008).
17 Monk, D., Arnaud, P., Apostolidou, S., Hills, F. A., Kelsey, G., Stanier, P. *et al.* Limited evolutionary conservation of imprinting in the human placenta. *Proc. Natl. Acad. Sci. USA.* **103,** 6623–6628 (2006).
18 Azzi, S., Rossignol, S., Steunou, V., Sas, T., Thibaud, N., Danton, F. *et al.* Multilocus methylation analysis in a large cohort of 11p15-related foetal growth disorders (Russell Silver and Beckwith Wiedemann syndromes) reveals simultaneous loss of methylation at paternal and maternal imprinted loci. *Hum. Mol. Genet.* **18,** 4724–4733 (2009).
19 Ogawa, H., Wu, Q., Komiyama, J., Obata, Y. & Kono, T. Disruption of parental-specific expression of imprinted genes in uniparental fetuses. *FEBS Lett.* **580,** 5377–5384 (2006).

Supplementary Information accompanies the paper on Journal of Human Genetics website (http://www.nature.com/jhg)

RESEARCH LETTER

AMERICAN JOURNAL OF medical genetics PART A

Reproductive Success in Patients With Hallermann–Streiff Syndrome

Hironao Numabe,[1,2] Hideaki Sawai,[2,3] Zentaro Yamagata,[4] Kaori Muto,[5] Rika Kosaki,[6] Kenya Yuki,[7] and Kenjiro Kosaki[8]*

[1]Department of Medical Ethics and Medical Genetics, Kyoto University Graduate School of Medicine, Kyoto, Japan

[2]Department of Clinical Genetics, Kyoto University Hospital, Kyoto, Japan

[3]Department of Obstetrics and Gynecology, Hyogo College of Medicine, Hyogo, Japan

[4]Department of Health Sciences, Interdisciplinary Graduate School of Medicine and Engineering, University of Yamanashi, Yamanashi, Japan

[5]Department of Public Policy, Human Genome Center, The University of Tokyo, Tokyo, Japan

[6]Division of Medical Genetics, National Center for Child Health and Development, Tokyo, Japan

[7]Department of Ophthalmology, Keio University School of Medicine, Tokyo, Japan

[8]Center for Medical Genetics, Keio University School of Medicine, Tokyo, Japan

Received 23 September 2010; Accepted 9 March 2011

How to Cite this Article:
Numabe H, Sawai H, Yamagata Z, Muto K, Kosaki R, Yuki K, Kosaki K. 2011. Reproductive success in patients with Hallermann–Streiff syndrome.
Am J Med Genet Part A 9999:1–3.

TO THE EDITOR:

Hallermann–Streiff syndrome (HSS) is characterized by premature aging, dyscephaly, hypotrichosis, microphthalmia, early-onset cataracts, a small pinched nose, micrognathia, and a proportionate short stature [Cohen, 1991]. HSS is a relatively rare condition: one survey of 27,472 newborns revealed only a single case of HSS [Higurashi et al., 1990]. After over five decades since its initial description, about 150 cases of HSS have been described in the literature; nevertheless, the genetic basis for this condition remains unknown. Most cases of HSS occur sporadically with no sex predilection. No cases of parent-to-child transmission have been reported except in one family [Koliopoulos and Palimeris, 1975], in which the diagnosis was challenged in an authoritative review of HSS [Cohen, 1991]. The extreme rarity of parent-to-child transmission suggests that HSS is transmitted in an autosomal recessive manner or that HSS represents an autosomal dominant disorder with markedly diminished reproductive fitness.

To date, a limited amount of information is available on the reproductive success of individuals with HSS. Previous reports of successful pregnancies in three female patients with HSS [Hendrix and Sauer, 1991; Cabral et al., 1994; Shiomi et al., 1999] in addition to one patient who was very briefly mentioned as having "two perfectly normal children" [Ponte, 1962] suggest the potential reproductive capacity of female patients. Here, we report a patient with HSS, who became pregnant and delivered unaffected children. Furthermore, a follow-up evaluation of a previously reported child born to an HSS female patient [Shiomi et al., 1999] revealed normal growth and development and is reported herein.

Patient 1

A 41-year-old woman was born to an 18-year-old mother at 41 weeks of gestation. Her birth weight was 3,050 g, her length was 49 cm, and her head circumference was 32 cm. Bilateral mandibular central incisors erupted at the age of 3 months. Respiratory distress occurred frequently during breastfeeding. At the age of 2 years, she was diagnosed as having HSS at the time of a cataract operation. At the age of 2 years and 9 months, her weight was 9,500 g, and her height was 83 cm. She had mild hypotrichosis, micrognathia, a narrow and highly arched palate, and atrophy of the skin. Menarche occurred at 13 years of age. At the age of 20 years, she became pregnant without the help of assisted reproductive technology. At age 21 years, she delivered an unaffected boy at 39 weeks of gestation after an uneventful pregnancy. The delivery was made by caesarean because of cephalopelvic disproportion. The birth weight of the

*Correspondence to:
Kenjiro Kosaki, M.D., Center for Medical Genetics, Keio University School of Medicine, 35 Shinanomachi, Shinjuku-ku, Tokyo 160-8582, Japan.
E-mail: kkosaki@z3.keio.jp
Published online 00 Month 2011 in Wiley Online Library (wileyonlinelibrary.com).
DOI 10.1002/ajmg.a.34042

child was 2,830 g, the length was 47 cm, and the head circumference was 32 cm all above the 10th centile. At that time, the patient's weight was 48 kg and her height was 143.7 cm (−2.5 SD). At age 25 years, she delivered an unaffected girl at 38 weeks of gestation after an uneventful pregnancy; the delivery was again by caesarean. The birth weight of the second child was 2,600 g, the length was 48 cm, and the head circumference was 31.5 cm. Her children are now 20 years and 16 years old, show no signs of HSS, and are healthy. The patient has suffered from glaucoma since the age of 35 years and has undergone three trabeculectomies. She also complains of general fatigue, palpitation, and obstructive sleep apnea, but these symptoms are not severe. Her present weight is 40 kg, and her height is 144 cm (−2.7 SD) (Fig. 1).

Patient 2

This patient was previously reported in a respiratory medicine journal in an article discussing the aggravation of obstructive sleep apnea during pregnancy [Shiomi et al., 1999]. Supplementary, corrected, and updated information was gathered with regard to the reproductive capacity of patients with HSS (Fig. 1).

A 38-year-old woman was born to a 24-year-old mother and a 31 -year-old father at 41 weeks of gestation. Her birth weight was 3,100 g, her length was 50 cm, and her head circumference was 31 cm. She was diagnosed as having HSS based on the development of cataracts, growth retardation, and dysmorphic features including brachycephaly, hypotrichosis, micrognathia, thin and pointed small nose, and high-arched palate. She suffered from glaucoma, anemia, chronic headache, and chronic neck and back pain. Menarche occurred at 15 years of age. At the age of 25 years, she became pregnant without the help of assisted reproductive technology. At the age of 26 years, she delivered a boy at 33 weeks of gestation. Recontact with the patient revealed that the gestational age at the time of delivery was 33 weeks, and not 36 weeks as originally reported by Shiomi et al. [1999]. The delivery occurred by caesarean because of impending obstructive sleep apnea, symphysiolysis, and breech presentation. The birth weight of the infant was 1,760 g (−0.6 SD, appropriate size for 33 weeks of gestation), the infant's length was 38 cm, and the head circumference was 30 cm. In the original report by Shiomi et al. [1999] the child was described as "a low birth weight infant" but no phenotypic information was given. Follow-up of the child revealed that he is presently 12 years old and has exhibited normal growth and development without any signs of HSS.

Here, we have reported on two patients with the classic features of HSS who became pregnant without the help of assisted reproductive technology, such as in vitro fertilization, and delivered phenotypically normal offspring. To better characterize the pregnancy histories of patients with HSS, we tabulated the clinical features of Patient 1 and Patient 2 together with those of three previously reported female patients with successful pregnancies (Table I). The table, which was constructed based on a retrospective review, does not prove, but suggests, that reproductive fitness may not be significantly impaired in female patients with HSS. On the other hand, it is unclear why only a limited number of individuals with HSS have been reported to bear children. Possible reproductive problems could be related to biological or sociological issues. To estimate the reproductive fitness in a quantitative manner, the number of children born to female HSS patients needs to be counted prospectively among patients who are planning to bear children.

None of the seven children born to mothers with HSS were affected. If HSS indeed represents an autosomal dominant disorder, a few affected children would carry the trait unless they die in utero. The lack of affected children does not exclude a dominant mode of inheritance, but certainly makes a dominant mode of inheritance less likely. On the other hand, the extreme rarity of sibling cases with

TABLE I. Successful Pregnancies in Female Patients With Hallermann–Streiff Syndrome

	Age at delivery (years)	Height (cm)	Gestational age at delivery (weeks)	Sex of the child	Birth weight of the child	Mode of delivery
Ponte et al. [1962]	NA	152	NA	NA (two children, both perfectly normal)	NA (two children, both perfectly normal)	NA (two children, both perfectly normal)
Hendrix et al. [1991]	NA	140	40	M	NA	CS
Cabral et al. [1994]	32	122	39	M	2,525 g (−1.3 SD)	CS due to CPD
Case 1						
1	21	143.7 (−2.7 SD)	39	M	2,830 g (−0.4 SD)	CS due to CPD
2	25		38	F	2,600 g (−0.6 SD)	CS due to previous CS
Case 2[a]	26	137 (−3.9 SD)	33	M	1,760 g (−0.6 SD)	CS due to obstructive sleep apnea, symphysiolysis, and breech presentation

CS, caesarean section; SD, standard deviation; CPD, cephalopelvic disproportion; NA, not available.

[a]Previously reported by Shiomi et al. [1999]. Recontact with the patient revealed that gestational age at delivery was 33 weeks, not 36 weeks as originally reported by Shiomi et al.

FIG. 1. Facial appearance of Patient 1 (left) and Patient 2 (right).

HSS does not favor a recessive mode of inheritance. Hence, the mode of inheritance remains unknown.

Since, HSS is characterized by premature aging, the mean age of delivery represents relevant information for female patients in terms of family planning. The mean age at the time of delivery among the four pregnancies in which the maternal age was known was 26.0 years. The intrauterine growth of the fetuses was age appropriate among the four pregnancies in which the birth weight was known; thus, the placental function of the affected mothers seems to have been maintained. Among the five pregnancies in which the gestational age at the time of delivery was known, four pregnancies lasted until at least 38 weeks, and cephalopelvic disproportion was thus anticipated. Indeed, among the five pregnancies in which the mode of delivery was known, all the pregnancies ended in delivery by caesarean section, presumably because of cephalopelvic disproportion associated with a short stature. Since a caesarean often requires general anesthesia and patients with HSS tend to have upper airway problems during and after general anesthesia, anticipatory anesthetic management is essential.

In summary, we report on two female patients with HSS who successfully became pregnant and delivered normal children. Documentation of the reproductive success of these patients further supports the potential reproductive capacity of women with HSS. This information will be valuable for individuals with HSS who are of child-bearing age and are making reproductive decisions.

ACKNOWLEDGMENTS

We thank the members of "Yui-yui," a Japanese Hallarmann–Streiff syndrome self-support group, for their kind information.

REFERENCES

Cabral CFJ, Orozco QM, Ibarguengoitia OF, Carballar LG, Karchmer S. 1994. Hallermann–Streiff syndrome and pregnancy. Report of a case. Ginecol Obstet Mex 62:207–210.

Cohen MMJ. 1991. Hallermann–Streiff syndrome: A review. Am J Med Genet 41:488–499.

Hendrix SL, Sauer HJ. 1991. Successful pregnancy in a patient with Hallermann–Streiff syndrome. Am J Obstet Gynecol 164:1102–1104.

Higurashi M, Oda M, Iijima K, Iijima S, Takeshita T, Watanabe N, Yoneyama K. 1990. Livebirth prevalence and follow-up of malformation syndromes in 27,472 newborns. Brain Dev 12:770–773.

Koliopoulos J, Palimeris G. 1975. A typical Hallermann–Streiff–Francois syndrome in three successive generations. J Pediat Ophthal 12:2359.

Ponte F. 1962. Further contributions to the study of the syndrome of Hallermann and Streiff (congenital cataract with "Bird's face"). Ophthalmologica 143:399–3408.

Shiomi T, Guilleminault C, Izumi H, Yamada S, Murata K, Kobayashi T. 1999. Obstructive sleep apnoea in a puerperal patient with Hallermann–Streiff syndrome. Eur Respir J 14:974–977.

RESEARCH ARTICLE

Human Mutation

OFFICIAL JOURNAL
HGVS
HUMAN GENOME VARIATION SOCIETY
www.hgvs.org

Disease-Associated Mutations in the Actin-Binding Domain of Filamin B Cause Cytoplasmic Focal Accumulations Correlating with Disease Severity

Philip B. Daniel,[1] Tim Morgan,[1] Yasemin Alanay,[2] Emilia Bijlsma,[3] Tae-Joon Cho,[4] Trevor Cole,[5] Felicity Collins,[6] Albert David,[7] Koen Devriendt,[8] Laurence Faivre,[9] Shiro Ikegawa,[10] Sebastien Jacquemont,[11] Milos Jesic,[12] Deborah Krakow,[13] Daniela Liebrecht,[14] Silvia Maitz,[15] Sandrine Marlin,[16] Gilles Morin,[17] Toshiya Nishikubo,[18] Gen Nishimura,[19] Trine Prescott,[20] Gioacchino Scarano,[21] Yousef Shafeghati,[22] Flemming Skovby,[23] Seiji Tsutsumi,[24] Margo Whiteford,[25] Martin Zenker,[26] and Stephen P. Robertson[1]*

[1]Department of Women's and Children's Health, Dunedin School of Medicine, Otago University, Dunedin, New Zealand; [2]Department of Pediatrics, Faculty of Medicine, Hacettepe University, Ankara, Turkey; [3]Department of Clinical Genetics, Leiden University Medical Center, Leiden, The Netherlands; [4]Division of Pediatric Orthopaedics, Seoul National University Children's Hospital, Seoul, Korea; [5]Clinical Genetics Unit, Birmingham Women's Hospital, Birmingham, B15 2TG, United Kingdom; [6]Department of Clinical Genetics, Children's Hospital at Westmead, Sydney, Australia; [7]Service de Génétique Médicale, Centre Hospitalier Universitaire, Nantes, France; [8]Centre for Human Genetics, University Hospital, K.U. Leuven, Leuven, Belgium; [9]Centre de Génétique, Hôpital d'Enfants, Dijon Cedex, France; [10]Laboratory for Bone and Joint Diseases, Center for Genomic Medicine, RIKEN, Tokyo, Japan; [11]Génétique Médicale, Centre Hospitalier Universitaire Vaudois, Lausanne, Switzerland; [12]Neonatology Department, University Children's Hospital, Belgrade, Serbia; [13]Medical Genetics Institute, Cedars-Sinai Medical Center and Departments of Orthopaedic Surgery and Human Genetics, UCLA, Los Angeles, California; [14]Pränatal-Medizin München, München, Germany; [15]Ambulatorio di Genetica Clinica Pediatrica, Clinica Pediatrica, Università Milano Bicocca A.O. S. Gerardo Fondazione MBBM, Monza, Italy; [16]Centre de Référence des Surdités Génétiques, Paris, France; [17]Unité de Génétique Clinique, Centre Hospitalier Universitaire d'Amiens, Amiens, France; [18]Division of Neonatal Intensive Care, Nara Medical University, Nara, Japan; [19]Department of Pediatric Imaging, Tokyo Metropolitan Children's Medical Center, Futyu, Japan; [20]Department of Medical Genetics, Oslo University Hospital, Oslo, Norway; [21]Birth Defects Registry of Campania, (BDRCam), Medical Genetics Unit, Gen. Hospital "G.Rummo", Benevento, Italy; [22]Medical Genetics Department, Sarem Women's Hospital, Tehran, Iran; [23]Department of Clinical Genetics, University Hospital of Copenhagen Rigshospitalet, Copenhagen, Denmark; [24]Department of Obstetrics and Gynecology, Yamagata University School of Medicine, Yamagata, Japan; [25]Ferguson-Smith Centre for Clinical Genetics, Yorkhill Hospitals, Glasgow, Scotland, United Kingdom; [26]Institute of Human Genetics, University Hospital of Magdeburg, Magdeburg, Germany

Communicated by Raymond Dalgleish

Received 23 June 2011; accepted revised manuscript 12 December 2011.
Published online 20 December 2011 in Wiley Online Library (www.wiley.com/humanmutation).DOI: 10.1002/humu.22012

ABSTRACT: Dominant missense mutations in *FLNB*, encoding the actin-cross linking protein filamin B (FLNB), cause a broad range of skeletal dysplasias with varying severity by an unknown mechanism. Here these *FLNB* mutations are shown to cluster in exons encoding the actin-binding domain (ABD) and filamin repeats surrounding the flexible hinge 1 region of the FLNB rod domain. Despite being positioned in domains that bind actin, it is unknown if these mutations perturb cytoskeletal structure. Expression of several full-length FLNB constructs containing ABD mutations resulted in the appearance of actin-containing cytoplasmic focal accumulations of the substituted protein to a degree that was correlated with the severity of the associated phenotypes. In contrast, study of mutations leading to substitutions in the FLNB rod domain that result in the same phenotypes as ABD mutations demonstrated that with only one exception disease-associated substitutions, surrounding hinge 1 demonstrated no tendency to form actin-filamin foci. The exception, a substitution in filamin repeat 6, lies within a region previously implicated in filamin-actin binding. These data are consistent with mutations in the ABD conferring enhanced actin-binding activity but suggest that substitutions affecting repeats near the flexible hinge region of FLNB precipitate the same phenotypes through a different mechanism.

Hum Mutat 00:1–9, 2012.

KEY WORDS: FLNB; FLNA; atelosteogenesis; boomerang dysplasia; Larsen syndrome

Introduction

Filamin proteins interact with the cytoskeleton by binding to filamentous actin (F-actin), and have the potential, through dimerisation, to crosslink actin fibrils [Cunningham et al., 1992; Hartwig and Stossel, 1975; Niederman et al., 1983]. In humans and mice, there are three filamin genes (*FLNA*; MIM# 300017, *FLNB*; MIM# 603381, and *FLNC*; MIM# 102565) with distinct expression patterns, but

Additional Supporting Information may be found in the online version of this article.

*Correspondence to: Stephen P. Robertson, Department of Women's and Children's Health, Dunedin School of Medicine, Otago University, Dunedin 9054, New Zealand. E-mail: stephen.robertson@otago.ac.nz

producing highly homologous proteins. In all three proteins, there is an amino terminal actin-binding domain (ABD), followed by 15 immunoglobulin-like filamin repeats (also referred to as rod domain 1), an hinge region (termed hinge 1), then eight more filamin repeats (rod domain 2), a second hinge region, and a final filamin repeat that mediates dimerisation.

Mutations in *FLNB*, the gene encoding filamin B (FLNB), cause a group of skeletal dysplasias, an observation that is consonant with expression of this protein in epiphyseal growth plate chondrocytes [Krakow et al., 2004]. Two broad groups of FLNB-related skeletal conditions can be defined on the basis of their clinical presentation and genetic etiology. Homozygosity or compound heterozygosity for null alleles results in the recessive condition spondylocarpotarsal syndrome (SCT; MIM# 272460), which features fusion of the vertebral, carpal, and tarsal bones. The phenotype observed for *Flnb*-null mice is consistent with the clinical features of SCT [Farrington-Rock et al., 2008; Lu et al., 2007; Zheng et al., 2007; Zhou et al., 2007]. A range of autosomal dominant diseases is caused by missense mutations or small in-frame deletions or insertions in *FLNB*. These phenotypes include atelosteogenesis I and III (AOI; MIM# 108720 and AOIII; MIM# 108721) and boomerang dysplasia (BD; MIM# 112310) that are severe disorders in which bones are either undermodeled or have failed to initiate ossification [Bicknell et al., 2005; Farrington-Rock et al., 2006]. Whereas AOIII is survivable in a minority of individuals, AOI and BD invariably present with in utero lethality. The least severe phenotype is Larsen syndrome (LS; MIM# 150250), which features joint dislocations and malformations of the cervical spine as well as supernumerary carpal and tarsal ossification centers [Bicknell et al., 2007].

A group of skeletal disorders with some phenotypic similarities to the *FLNB* group of disorders has also been linked to clustered missense mutations in the paralogous gene *FLNA*, which encodes the protein filamin A [Robertson et al., 2003]. Some of these mutations occur at amino acids homologous to those causing the LS-AO-BD spectrum of conditions in *FLNB*. Similar to *FLNB*, these diseases are clinically distinct from the disease resulting from loss-of-function mutations in *FLNA* [Robertson, 2005].

How some missense mutations in *FLNA* and *FLNB* lead to skeletal disease is uncertain. The ability to crosslink F-actin indicates a structural role in the cytoskeleton, but interactions detected with dozens of other proteins including integrins, transmembrane receptors, and transcription factors also suggest a role in scaffolding mediators of multiple other cellular processes [Nakamura et al., 2011]. Latterly, a role for filamins in mechanosensation has also been established with evidence accumulating that filamin A has the ability to convert biomechanical stress sensed via integrins into a chemical signal mediated by small GTPases [Ehrlicher et al., 2011]. The prominent skeletal phenotypic manifestations of the dominantly inherited LS-AO-BD disorders also raise the possibility that disruption of the mechanosensory properties of filamins may relate to the pathogenesis of these developmental conditions [Mammoto and Ingber, 2010]. Filamin-integrin interactions can be modulated by extrinsic force [Ehrlicher et al., 2011; Kiema et al., 2006b; Lad et al., 2007b] and deletion of hinge 1, the structure that confers flexibility to the filamin rod domain, thereby altering the mechanosensory properties of these proteins [Gardel et al., 2006]. It is conceivable therefore that filamin-actin binding may be physiologically modulated to achieve the same end and that gain-of-function missense mutations in *FLNA* [Clark et al., 2009] and *FLNB* [Sawyer et al., 2009] may impact on cellular mechanotransduction by conferring an increase in actin-filamin avidity. Relevant to these many cellular roles, actin-bound filamin transitions between many cellular compartments including the cortical cytoskeleton, actin stress fibers, and a newly recognized perinuclear structure called the actin cap [Gay et al., 2011]. Although some modulators of actin-filamin binding have been identified [Nakamura et al., 2005], a comprehensive understanding of the in vivo regulation of actin-filamin transitions is still lacking.

The ABD of filamins comprises two calponin homology subdomains (CH1 and CH2) arranged in tandem. The CH2 is proposed to regulate F-actin binding mediated by CH1 [Lorenzi and Gimona, 2008], a model supported by the observation that deletion of CH2 from ABD constructs leads to focal accumulation of these proteins bound to actin, [Lorenzi and Gimona, 2008]. Significantly, missense mutations in the ABD of FLNB that lead to the LS-AO-BD spectrum of conditions occur only in CH2 and not CH1 [Bicknell et al., 2007; Farrington-Rock et al., 2006; Krakow et al., 2004]. These mutations confer an increased avidity to the actin-filamin binding interaction [Sawyer et al., 2009] providing strong evidence for dysregulation of actin-filamin interactions as the key mechanism underlying these conditions.

Here the cytoskeletal consequences of dominant missense mutations in FLNB that lead to the LS-AO-BD spectrum of conditions is studied by cataloguing the distribution of mutations that lead to these disorders over the gene and examining the effect of expressing full length GFP-labeled mutation-containing FLNB on its intracellular distribution and actin cytoskeletal architecture. We conclude that the nonrandom clustering of LS-AO-BD disease-causing mutations is indicative of at least two pathogenic mechanisms of generating these disease phenotypes; one of which relates to enhanced actin binding and bundling and the other possibly dysregulating the function of hinge 1.

Methods and Materials

Human Subjects and Mutation Detection

All subjects were ascertained by physician-initiated referral and consented to participate under an institutional protocol approved by the Otago Ethics Committee. The clinical and radiographic phenotypes were reviewed by one of us (SR) to ensure the diagnoses were correctly assigned according to previously published criteria [Bicknell et al., 2007; Farrington-Rock et al., 2006]. The exon and intron–exon boundaries of *FLNB* were amplified by polymerase chain reaction (PCR) using previously published primers [Krakow et al., 2004] and subjected to denaturing high performance liquid chromatography (DHPLC) using the WAVE platform (Transgenomic, Omaha, NE) or using direct sequencing on an ABI3100 capillary sequencer as previously described [Bicknell et al., 2007]. Nucleotide numbering reflects cDNA numbering with +1 corresponding to the A of the ATG translation initiation codon in the reference sequence NM_001457.3. For protein numbering, the initiation codon is denoted codon 1. Mutations are referred to in the text by the inferred amino acid substitution.

Plasmid Constructs

The full-length FLNB cDNA clones used in these studies (pCMV-FLNB and pCMV-FLNB-EGFP) were assembled by PCR from M2 melanoma cell line cDNA and pCI-FLNB-EGFP [van der Flier et al., 2002], in the expression vector pCR3.1(-) (Invitrogen, Carlsbad, CA). The clones are concordant with reference sequence NM_001457.3. PCR mutagenesis was performed using forward and reverse oligonucleotide primers containing the single-nucleotide

alteration, paired with 5′ and 3′ external primers. Products were subcloned into pCMV-FLNB or pCMV-FLNB-EGFP using the restriction enzymes *Xba*I (in pCR3.1[-]) and *Bam*HI (NT 2175). Primers and further details are available on request.

For mutations in repeat 6 (p.Gly751Arg), repeat 14 (p.Ser1602Pro), and repeat 15 (p.Pro1699Ser), subcloning was performed using the *Bam*HI (NT 2176) and *Sac*II (NT 6195) sites. The presence of expected mutations was confirmed by sequencing over the subcloned regions, and two or more independent clones for each mutant were compared in transfection experiments. All PCR was carried out with *Pwo* polymerase (Roche Diagnostics GmbH, Mannheim, Germany).

Transfection

HEK293 cells were grown in DMEM + 10% FCS. For transfection, cells were seeded in 24-well plates at 20,000 cells per well on gelatin-coated coverslips. Transfection was performed the following day with 200 ng of DNA and 0.6 μl of Fugene (Roche) per well. Cells were analyzed at 48 hr post-transfection. The DsRed-monomer-actin construct (Clontech, Mountain View, CA) was used in cotransfections at 20 ng per well cotransfected with 80 ng of FLNB expression construct per well. M2 cells were grown in alpha MEM + 8% NCS and 2% FCS. For transfection, cells were seeded in 24-well plates at 50,000 cells per well on gelatin-coated coverslips. Antibiotic-free media was used for pretransfection plating. Transfection was carried out either immediately with the cells in suspension, or the following day with 400 ng of DNA and 1 μl of Lipofectamine 2000 (Invitrogen) per well. Cells were used at 48 hr post-transfection. DNA used in transfections was prepared using either maxiprep kits (Qiagen, Hilden, Germany) or alkaline lysis minipreps further purified with Qiagen PCR purification columns.

Immunodetection and Imaging

Cells on coverslips were fixed with 1% paraformaldehyde in PBS for 5 min and then rinsed once in PBS. For imaging of EGFP constructs, cells were incubated with 10μg/ml 4′,6-diamidino-2-phenylindole (DAPI) for 10 min. Coverslips were rinsed in 0.1× PBS and mounted inverted on slides with Glycergel (Dako, Glostrup, Denmark). For immunocytochemistry, cells were permeabilized with PBS containing 0.2% triton X-100 and 5% bovine serum albumin (BSA) and rinsed once in PBS. Primary antibodies were applied in PBS + 1% BSA at the following concentrations: Rabbit polyclonal anti-FLNB (AB9276; Chemicon, Temecula, CA) at 1:400 dilution; mouse monoclonal anti-FLNA (MAB1678, Chemicon) at 1:1,000 dilution.

To visualize the actin cytoskeleton, Alexafluor 350-phalloidin (Molecular Probes, Eugene, OR) was applied to permeabilized BSA-blocked cells at a concentration of 1 unit in 250 μl of PBS + 1% BSA for 30 min. Cells were incubated 30 min and then rinsed twice for 3 min with PBS. Secondary antisera (goat anti-rabbit IgG-Alexafluor594 conjugate or goat antimouse IgG Alexafluor488 conjugate, (Molecular Probes)) were applied at 1:400 dilution in PBS +1% BSA for 30 min followed with two rinses of PBS, 3 min each. Cells were stained with DAPI and mounted as described above. Analysis and image capture was performed on a Zeiss Axioplan microscope fitted with a 1.39 megapixel CCD camera (Diagnostic Instruments, Sterling Heights, MI). Images were captured and processed with Spot 4.6 (Diagnostic Instruments) and Adobe Photoshop 10.0 software (Adobe Systems Incorporated, San Jose, CA).

Western blots were carried out with rabbit anti-GFP antisera (Invitrogen) at 1:100 dilution.

Results

Distribution of Mutations Underlying the LS-AO-BD Spectrum of Disorders

Genomic DNA samples obtained from 67 patients with a diagnosis of LS, AOI/III, or BD had a causative mutation found by sequencing of all exons and intron–exon boundaries of *FLNB*. The mutations found in these individuals together with those previously reported to underlie these phenotypes [Bicknell et al., 2005; Bicknell et al., 2007; Farrington-Rock et al., 2006; Krakow et al., 2004] are reported in Table 1. Criteria for determination of pathogenicity for mutations included segregation with the phenotype, a demonstration that the causative variant had arisen de novo in the context of sporadic disease in the offspring of otherwise healthy parents and alteration of evolutionarily conserved residues in the parent protein as previously described (*ibid*).

As previously noted for these conditions, all mutations ($n = 72$) were either missense mutations or small in-frame deletions that are predicted to preserve the reading frame and production of full-length protein. Figure 1A depicts the distribution of these mutations mapped onto the corresponding domains of the FLNB protein. Mutations leading to these disorders are distributed in a highly non-random fashion with clusters of mutations found in exons encoding the CH2 portion of the ABD and repeats 14 to 17, flanking hinge 1. Mutations leading to phenotypes spanning the full range of severity were found represented in both mutation clusters, with the exception of BD, which is caused solely by substitutions within CH2.

Detailed analysis of the distribution of mutations in the CH2 subdomain demonstrated that although some mutations were observed recurrently, substitutions with pathogenic outcomes were distributed widely over the entirety of CH2 (Fig. 1B). A similar analysis of mutations in *FLNA* that lead to a spectrum of skeletal dysplasias called the otopalatodigital syndrome spectrum disorders showed a similar distribution of mutations within the CH2 subdomain [Robertson, 2005]. This observation indicates that the pathogenic effect conferred by amino acid substitutions with the CH2 subdomain of these proteins can be conferred by a broad range of mutations affecting this localized region of the molecule and suggests a pathophysiological mechanism analogous to the functional inactivation of the CH2 subdomain in the absence of significant structural disruption [Sawyer et al., 2009]. The actin-binding activity within the ABD is known to reside with CH1 although the presence of a CH2 subdomain in tandem with this subdomain appears to modulate actin-binding activity [Lorenzi and Gimona, 2008]. Consequently, the effect of these naturally arising substitutions was examined by transfection and expression of constructs bearing a selection of these mutations in HEK293 and in M2 cells, a cell line that lacks endogenous *FLNA* expression.

BD Mutation p.Ser235Pro Results in Cytoplasmic Focal Accumulations

When full-length FLNB is expressed in HEK293 cells, it is extensively distributed within the cytoplasm (Fig. 2A, panels *a* and *d*). This distribution has the appearance of a fine meshwork, consistent with binding to the actin cytoskeleton. This is in contrast to endogenous FLNB in untransfected cells (Supp. Fig. S1), which has a less even distribution featuring distinct accumulations in perinuclear areas. The ectopic FLNB distribution resembles that of endogenous FLNA (Fig. 2A, panels *b* and *e* and Supp. Fig. S1), filling the cytoplasm and filopodial extensions. The ectopic FLNB colocalizes with, rather than displaces, FLNA.

Table 1. Distribution of *FLNB* Mutations among 67 Patients Diagnosed with LS, AOI/III, or BD

Diagnosis	Mutation	Protein	*N*	Origin	Protein domain	Reference
Boomerang dysplasia	c.512T>G	p.(Leu171Arg)	1	De novo	CH2	Bicknell et al., [2005]
Boomerang dysplasia	c.605T>C	p.(Met202Thr)	1	Unknown	CH2	
Boomerang dysplasia	c.703T>C	p.(Ser235Pro)	1	Unknown	CH2	Bicknell et al., [2005]
Atelosteogenesis I	c.442T>A	p.(Trp148Arg)	1	Unknown	CH2	Farrington-Rock et al., [2006]
Atelosteogenesis I	c.447_458del	p.(Gln150_Ile153del)	1	De novo	CH2	
Atelosteogenesis I	c.495G>T	p.(Trp165Cys)	1	De novo	CH2	
Atelosteogenesis I	c.502G>A	p.(Gly168Ser)	2	De novo	CH2	
Atelosteogenesis I	c.503G>T	p.(Gly168Val)	1	De novo	CH2	
Atelosteogenesis I	c.512T>A	p.(Leu171Gln)	1	Unknown	CH2	Farrington-Rock et al., [2006]
Atelosteogenesis I	c.518C>T	p.(Ala173Val)	1	Unknown	CH2	Krakow et al., [2004]
Atelosteogenesis I	c.542G>T	p.(Gly181Val)	1	Unknown	CH2	Farrington-Rock et al., [2006]
Atelosteogenesis I	c.549C>G	p.(Cys183Trp)	1	Unknown	CH2	Farrington-Rock et al., [2006]
Atelosteogenesis I	c.562T>C	p.(Ser188Pro)	1	De novo	CH2	Krakow et al., [2004]
Atelosteogenesis I	c.565T>G	p.(Trp189Gly)	1	Unknown	CH2	
Atelosteogenesis I	c.565T>C	p.(Trp189Arg)	1	De novo	CH2	
Atelosteogenesis I	c.604A>G	p.(Met202Val)	2	Unknown	CH2	Krakow et al., [2004]
Atelosteogenesis I	c.608A>C	p.(Gln203Pro)	1	Unknown	CH2	Farrington-Rock et al., [2006]
Atelosteogenesis I	c.613G>A	p.(Ala205Thr)	1	De novo	CH2	
Atelosteogenesis I	c.4737_4738insC; 4746_4758del	p.(Tyr1580Leu;Ile1581His; Asp1583_Gly1586del)	1	Unknown	Repeat 14	Farrington-Rock et al., [2006]
Atelosteogenesis I	c.4747_4749del	p.(Asp1583del)	1	Unknown	Repeat 14	Farrington-Rock et al., [2006]
Atelosteogenesis I	c.4804T>C	p.(Ser1602Pro)	1	Unknown	Repeat 14	Farrington-Rock et al., [2006]
Atelosteogenesis I	c.5095C>T	p.(Pro1699Ser)	1	Unknown	Repeat 15	
Atelosteogenesis III	c.500A>T	p.(Asp167Val)	1	De novo	CH2	
Atelosteogenesis III	c.502G>A	p.(Gly168Ser)	4	Inherited (Mosaic parent)	CH2	Farrington-Rock et al. [2006]
Atelosteogenesis III	c.502G>T	p.(Gly168Cys)	1	Unknown	CH2	
Atelosteogenesis III	c.602C>T	p.(Asp201Val)	1	Unknown	CH2	Farrington-Rock et al., [2006]
Atelosteogenesis III	c.604A>G	p.(Met202Val)	1	De novo	CH2	Krakow et al., [2004]
Atelosteogenesis III	c.629G>T	p.(Gly210Val)	1	Unknown	CH2	Farrington-Rock et al., [2006]
Atelosteogenesis III	c.1087G>A	p.(Gly363Arg)	1	De novo	Repeat 2	
Atelosteogenesis III	c.2055+1G>A	p.(Q685_686ins9)	1	Unknown	Repeat 5	
Atelosteogenesis III	c.2251G>C	p.(Gly751Arg)	1	De novo	Repeat 6	Krakow et al., [2004]
Atelosteogenesis III	c.4835G>A	p.(Gly1612Asp)	1	Unknown	Repeat 15	Farrington-Rock et al., [2006]
Atelosteogenesis III	c.4927G>C	p.(Ala1643Pro)	1	Unknown	Repeat 15	Farrington-Rock et al., [2006]
Atelosteogenesis III	c.5071G>A	p.(Gly1691Ser)	3	Unknown	Repeat 15	Farrington-Rock et al., [2006]
Atelosteogenesis III	c.5074G>A	p.(Gly1692Ser)	1	De novo	Repeat 15	
Larsen syndrome	c.482T>G	p.(Phe161Cys)	3	Inherited	CH2	Krakow et al., [2004]
Larsen syndrome	c.488A>C	p.(Gln163Pro)	1	Unknown	CH2	
Larsen syndrome	c.501C>A	p.(Asp167Glu)	1	De novo	CH2	
Larsen syndrome	c.500A>G	p.(Asp167Gly)	1	De novo	CH2	
Larsen syndrome	c.502G>A	p.(Gly168Ser)	2	Inherited	CH2	Bicknell et al., [2007]
Larsen syndrome	c.572C>T	p.(Pro191Leu)	1	De novo	CH2	
Larsen syndrome	c.590A>T	p.(Asn197Ile)	1	Unknown	CH2	
Larsen syndrome	c.622T>C	p.(Trp208Arg)	1	De novo	CH2	
Larsen syndrome	c.661A>T	p.(Ile221Phe)	1	Unknown	CH2	
Larsen syndrome	c.679G>A	p.(Glu227Lys)	15	Inherited	CH2	Krakow et al., [2004]
Larsen syndrome	c.685T>C	p.(Ser229Pro)	1	Unknown	CH2	
Larsen syndrome	c.700C>G	p.(Leu234Val)	1	De novo	CH2	Bicknell et al., [2007]
Larsen syndrome	c.1081G>A	p.(Gly361Ser)	1	De novo	Repeat 2	Bicknell et al., [2007]
Larsen syndrome	c.1081G>T	p.(Gly361Cys)	1	Unknown	Repeat 2	
Larsen syndrome	c.1082G>A	p.(Gly361Asp)	2	Unknown	Repeat 2	
Larsen syndrome	c.1088G>A	p.(Gly363Glu)	1	De novo	Repeat 2	Bicknell et al., [2007]
Larsen syndrome	c.4292T>G	p.(Leu1431Arg)	1	De novo	Repeat 13	Bicknell et al., [2007]
Larsen syndrome	c.4580T>A	p.(Leu1527His)	1	Unknown	Repeat 14	
Larsen syndrome	c.4580T>C	p.(Leu1527Pro)	1	De novo	Repeat 14	
Larsen syndrome	c.4621G>C	p.(Ala1541Pro)	1	De novo	Repeat 14	
Larsen syndrome	c.4625T>C	p.(Ile1542Thr)	2	Unknown	Repeat 14	
Larsen syndrome	c.4711_4713del	p.(Asn1571del)	1	De novo	Repeat 14	Krakow et al., [2004]
Larsen syndrome	c.4725_4736del	p.(Ala1577_Tyr1580del)	1	Unknown	Repeat 14	
Larsen syndrome	c.4756G>A	p.(Gly1586Arg)	2	De novo	Repeat 14	Krakow et al., [2004]
Larsen syndrome	c.4775T>A	p.(Val1592Asp)	2	Inherited	Repeat 14	Bicknell et al., [2007]
Larsen syndrome	c.4781A>C	p.(Tyr1594Ser)	1	De novo	Repeat 14	
Larsen syndrome	c.4795A>T	p.(Ile1599Phe)	1	Unknown	Repeat 14	
Larsen syndrome	c.4805C>A	p.(Ser1602Tyr)	1	Unknown	Repeat 14	
Larsen syndrome	c.4808C>T	p.(Pro1603Leu)	1	De novo	Repeat 14	
Larsen syndrome	c.4936G>A	p.(Gly1646Ser)	1	Unknown	Repeat 15	
Larsen syndrome	c.5023_5025del	p.(Phe1675del)	1	Unknown	Repeat 15	
Larsen syndrome	c.5071G>A	p.(Gly1691Ser)	9	Unknown	Repeat 15	Krakow et al., [2004]
Larsen syndrome	c.5071G>T	p.(Gly1691Cys)	1	Unknown	Repeat 15	
Larsen syndrome	c.5072G>A	p.(Gly1691Asp)	1	De novo	Repeat 15	
Larsen syndrome	c.5500G>A	p.(Gly1834Arg)	2	De novo	Repeat 17	Bicknell et al., [2007]
Larsen syndrome	c.5706C>A	p.(Ser1902Arg)	1	De novo	Repeat 17	
Larsen syndrome	c.7290_7313del	p.(Cys2431_Tyr2438del)	1	Unknown	Repeat 23	

Origin: "Inherited" if any case of parental transmission is confirmed; "De novo" if any parents of patients are confirmed noncarriers, and no inherited examples are known; "Unknown" if parental DNA has not been examined. Mutation numbering relates to the reference sequence NM_001457.3 with the +1 position referring to the A of the initator methionine codon.

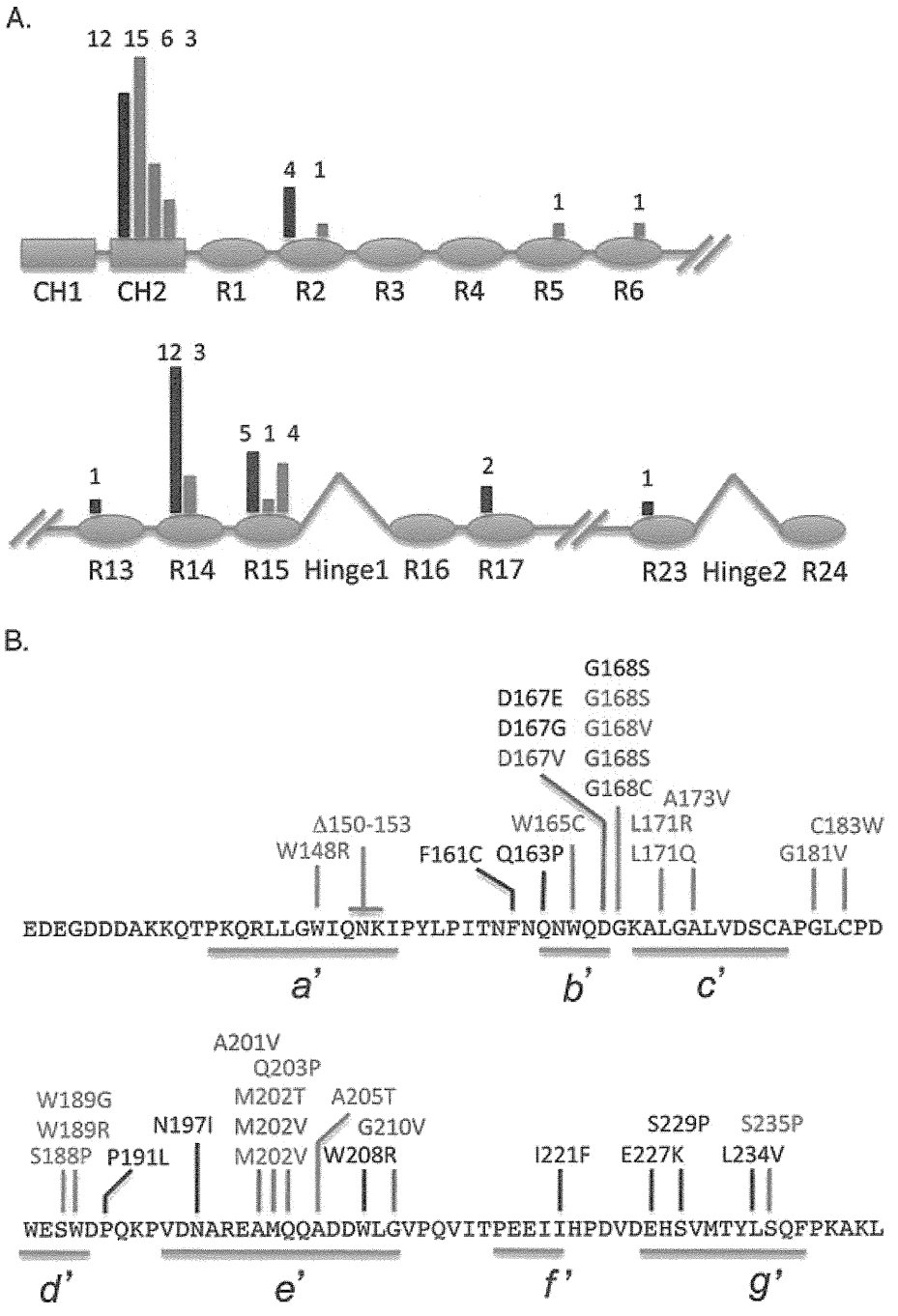

Figure 1. Dominant mutations in *FLNB* leading to the LS-AO-BD spectrum of skeletal dysplasias. **A**: Schematic of FLNB indicating the sites and frequencies of mutations underlying the LS-AO-BD spectrum. Column height denotes frequency within the associated domain or subdomain (actual numbers are given above the columns), while column color denotes disease association as follows: LS (black), AOI (green), AOIII (blue), BD (red). **B:** Distribution of mutations in FLNB CH2 subdomain. Disease associations are color-coded as in A. Recognized α-helices are underlined and identified with a letter (the prime is added to distinguish CH2 helices from helices in CH1).

When transfected FLNB contained the mutation p.Ser235Pro, (causative of the most severe FLNB-related disease, BD), the distribution of FLNB became concentrated in globular accumulations of varying sizes (panel *g* and *j*), or in some cases, networks of thickened fibrils (panel *m*). These globular foci also contain FLNA (panels *h*, *k*, *n* and merged in *i*, *l*, and *o*).

Similar results were seen with FLNB-EGFP fusion proteins (Fig. 2B). FLNB-EGFP occupied the entire cytoplasm (panels *a* and *b*) whereas FLNB^{Ser235Pro}-EGFP was largely restricted to globular foci and thickened fibrils (*c* and *d*). A rare example of punctate distribution for FLNB-EGFP is seen in panel *b*.

Since these experiments and other work [Sheen et al., 2002] have suggested colocalization and possible heterodimerisation of FLNA and FLNB, it was necessary to determine whether the presence of FLNA was required for the formation of foci. To answer this question M2, a human melanoma cell line that lacks FLNA expression,

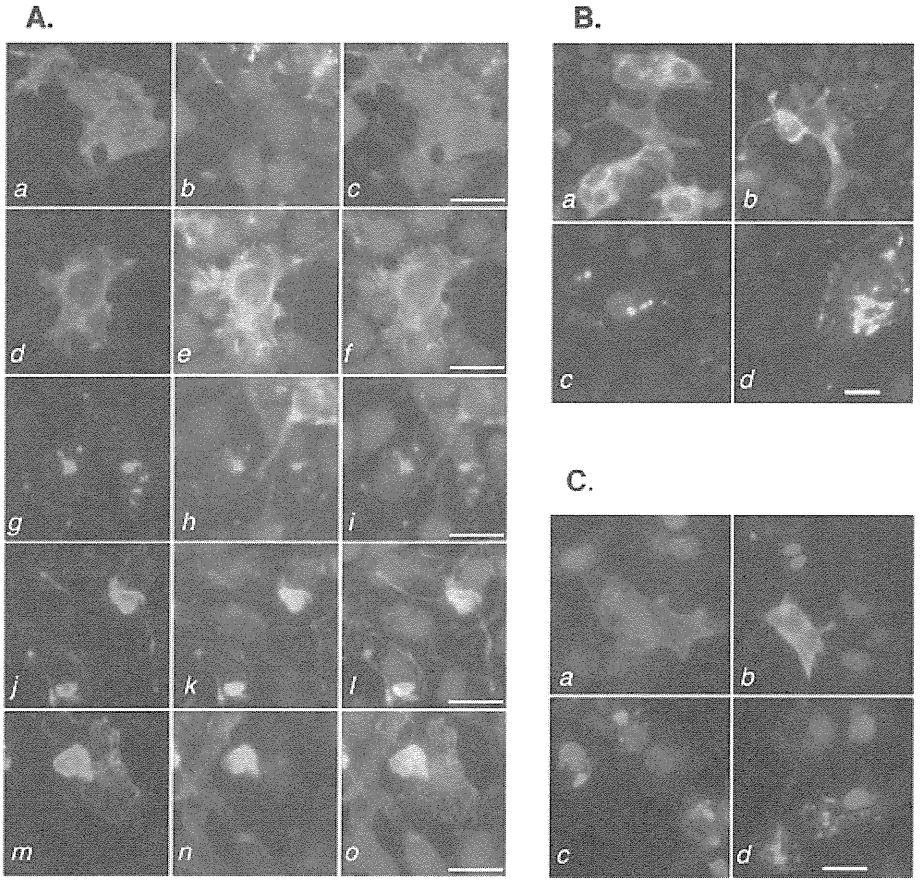

Figure 2. Detection of FLNB protein in transfected cells and effects of mutations on cellular localization. **A:** HEK293 cell line transfected with pCMV-FLNB (*a-f*) or pCMV-FLNB^{Ser235Pro} (*g-o*) analyzed for FLNB and FLNA expression by immunofluorescence. Images are of FLNB signal (red; *a, d, g, j, m*; gamma adjustment 2), FLNA signal (green; *b, e, h, k, n*; gamma adjustment 2), and both signals digitally merged with DAPI (blue) (*c, f, i, l, o*). Scale bars 20 μM. **B:** HEK293 cell line transfected with pCMV-FLNB-EGFP (*a, b*) or pCMV-FLNB^{Ser235Pro}-EGFP (*c, d*) analyzed for EGFP expression (green; gamma adjustment 2) merged with DAPI (blue). Scale bar 20 μM. **C:** M2 melanoma cell line transfected with pCMV-FLNB (*a, b*) or pCMV-FLNB^{Ser235Pro} (*c, d*) analyzed for FLNB expression by immunofluorescence (red; gamma adjustment 2), digitally merged with DAPI (blue). Scale bar 20 μM.

was transfected with the same constructs. In these experiments, the disparate patterns of FLNB and FLNB^{Ser235Pro} localization still occurred (Fig. 2C, panels *a* and *b* compared to panels *c* and *d*). This indicates that the foci do not occur because of FLNA displacing mutant FLNB through competition for actin binding, nor is FLNA required as a heterodimerisation partner.

FLNB^{Ser235Pro} Foci Contain Actin

The p.Ser235Pro substitution occurs within the CH2 portion of the ABD of FLNB. It is conceivable that any mutation altering the structure of the ABD may prevent the association of FLNB with the actin cytoskeleton. To address this possibility, changes in the distribution of actin in the presence of mutant FLNB were investigated. In cells cotransfected, with wild-type or mutant FLNB and DsRed-tagged actin (Fig. 3A), it can be seen that actin accumulates at the foci. Similar results are seen in cells transfected with wild-type or mutant FLNB and stained with phalloidin-Alexafluor conjugate (Fig. 3B). This observation is consistent with the hypothesis that the p.Ser235Pro mutation does not abrogate actin binding. Cytoskeletal actin was also detected outside of the foci in transfected cells, indicating that the actin cytoskeleton was not entirely disrupted. Similar results were observed in experiments that utilized M2 cells (Supp. Fig. S2), showing that FLNA was not required for inclusion of actin in the foci through heterodimer formation [Sheen et al., 2002]. FLNB-EGFP wild-type and mutant expression constructs were also examined for evidence of degradation by transfection and Western blot (Fig. 3C and Supp. Fig. S3). All constructs were found to express at similar levels, and no degradation products were observed, even on longer exposure. This indicates that the foci are comprised of intact FLNB.

The Extent of Focal Accumulation Correlates with Disease Severity

To examine whether the focal accumulation of FLNB might occur in other mutant forms of FLNB, other CH2 mutations were introduced into the FLNB-EGFP fusion protein construct. Mutations resulting in substitutions p.Leu171Arg (BD), p.Tyr148Arg (AOI), p.Met202Val (AOI and AOIII), p.Glu227Lys (LS), and p.Phe161Cys (LS) were all found to cause focal accumulation of the fusion protein in HEK293 cells (Fig. 4). Significantly, there was variability in the extent of focal accumulation. Similar to p.Ser235Pro, the p.Leu171Arg mutation left almost no cytoplasmic signal outside of the globular

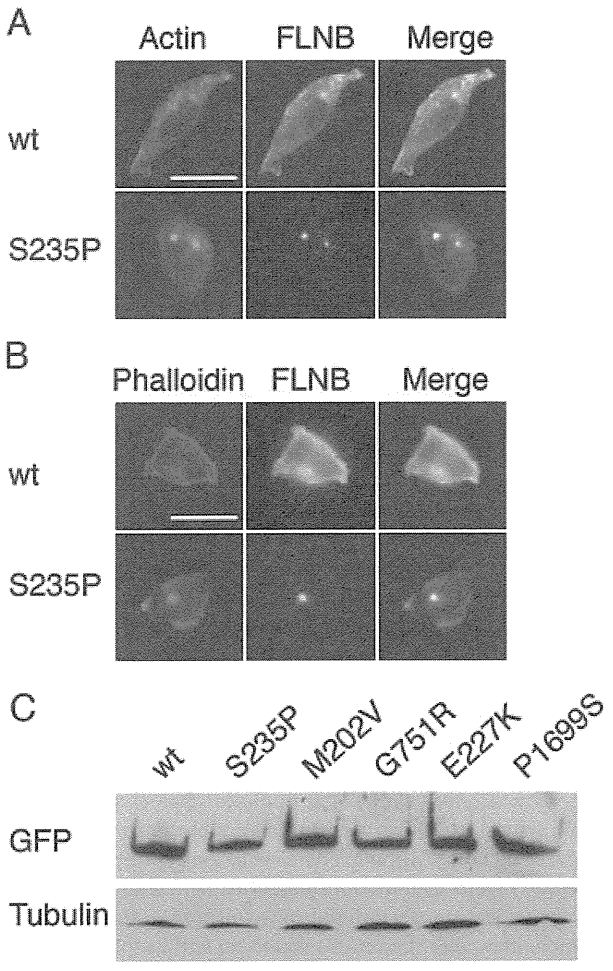

Figure 3. Colocalization of actin and FLNB^{Ser235Pro}. **A:** HEK293 cell line transfected with pCMV-FLNB or pCMV-FLNB^{Ser235Pro} and cotransfected with DsRed-actin. Scale bar 20 μM. **B:** HEK293 cell line transfected with pCMV-FLNB or pCMV-FLNB^{Ser235Pro} and stained with Alexafluor 350-phalloidin. Scale bar 20 μM. **C.** Western blot of pCMV-FLNB-EGFP constructs (wild-type or bearing indicated mutations) probed with anti-GFP antisera and an anti-β-tubulin control.

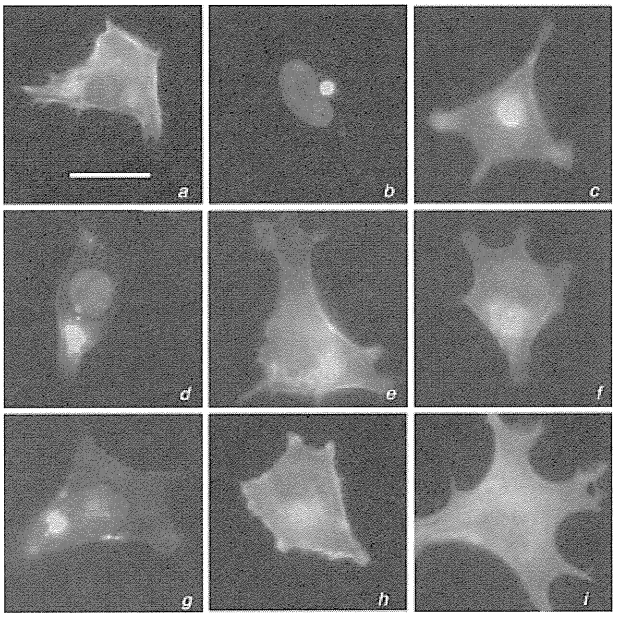

Figure 4. Cellular localization of EGFP-tagged FLNB constructs bearing mutations causative of the BD-AO-LS disorders. HEK293 cell line transfected with pCMV-FLNB-EGFP fusion constructs carrying CH2 mutations and analyzed for EGFP expression (green; gamma adjustment 2) digitally merged with DAPI (blue). Wild-type FLNB (*a*) is compared to FLNB with substitutions p.Leu171Arg (*b*), p.Met202Val (*c*), p.Tyr148Arg (*d*), p.Glu227Lys (*e*), p.Phe161Cys (*f*), p.Gly751Arg (*g*), p.Ser1602Pro (*h*), and p.Pro1699Ser (*i*). Scale bar 20 μM.

foci (Fig. 4, panel *b*). Both p.Met202Val (panel *c*) and p.Tyr148Arg (panel *d*) while producing foci in the vast majority of transfected cells also displayed more general cytoplasmic localization. The distribution of FLNB-EGFP constructs containing p.Glu227Lys and p.Phe161Cys substitutions frequently resembled that of cells transfected with wild-type fusion protein, or showed only minor focal accumulations (panels *e* and *f*). Thickened fibrils were also observed in some p.Glu227Lys transfectants (Supp. Fig. S4A, panel *j*). Similar results were obtained with M2 cells (Supp. Fig. S4B).

Disease-Associated FLNB Mutations in Repeats 14 and 15 do not Lead to Formation of Filamin-Actin Foci

Mutations outside the ABD also result in identical disease phenotypes as those caused by mutations within the CH2 region (Fig. 1 and Table 1). The mutations are mostly clustered with the repeats flanking hinge 1 but are also occasionally seen at residues remote from this region (Fig. 1A). To determine if the focal accumulation phenomenon was restricted to mutations leading to CH2 substitutions, three amino acid substitutions from repeat 6 (p.Gly751Arg; AOIII), repeat 14 (p.Ser1602Pro; AOIII), and repeat 15 (p.Pro1699Ser; severe AOI) were introduced into the FLNB-EGFP fusion construct and transfected into HEK293 cells (Fig. 4, panels *g–i*). While the p.Gly751Arg mutant showed good evidence of foci formation (panel *g*), equivalent to other AOI/III mutations, the p.Ser1602Pro and p.Pro1699Ser mutants did not differ markedly from the wild-type fusion protein distribution (panels *h* and *i*, respectively). Similar results were seen utilizing M2 cells to rule out any confounding influence that FLNA expression might have upon these observations (Supp. Fig. S4B).

Discussion

Several lines of evidence indicate that the pathogenic mechanism underlying the autosomal dominant spectrum of disorders due to mutations in *FLNB* that includes BD, AOI/III, and LS is distinct from the recessively inherited disorder SCT. First, the diseases caused by recurrent and clustered amino acid substitutions within the CH2 subdomain and first rod domain of FLNB are quite distinct phenotypically from SCT syndrome that results from truncating mutations leading to loss of expression of this protein [Farrington-Rock et al., 2008]. Additionally, heterozygous carriers for SCT mutations exhibit minimal or no skeletal manifestations, indicating that the BD-AO-LS spectrum is unlikely to be due to haploinsufficiency at the *FLNB* locus. Third, recent data indicate that mutations within the ABD leading to the BD-AO-LS spectrum of conditions lead to increased F-actin avidity in the absence of structural destabilization of this domain [Sawyer et al., 2009] as do analogous mutations

in *FLNA* [Clark et al., 2009] and *FLNC* [Duff et al., 2011]. Together these observations indicate a gain-of-function is conferred by mutations leading to BD-AO-LS but equally there remains little mechanistic understanding of the cellular consequences of the increase in actin-binding capability conferred by these alleles.

The data presented here link several lines of evidence to suggest that mutations that lead to enhanced actin binding do so by disabling CH2 regulatory function and that the result is abnormal transitioning of FLNB between networks and bundles of actin fibers. Although previously in vitro evidence demonstrated that the CH2 subdomain negatively regulates actin avidity and binding, a demonstration that this affects full-length filamin function and what the downstream consequences were on cell remain unexplored. In transient transfection experiments, BD-causing mutations in FLNB (p.Ser235Pro and p.Lys171Arg) led to nearly complete localization of the mutant proteins within actin containing cytoplasmic focal accumulations. These foci are not observed with overexpression of the wild-type protein and are unlikely to represent nonspecific aggregation of substituted protein, since they colocalize with actin and FLNA. Equally, the observed foci are unlikely to represent aggregation of degraded protein, since Western analysis of transfected cells revealed little evidence for this and filamin A would be unlikely to colocalize with mutant protein that had been directed to the proteosome. Recently, FLNA has been shown to regulate the formation of an analogous actin-rich perinuclear body, termed the actin cap [Gay et al., 2011], a transient structure that relates to regulated alterations in nuclear location and shape.

Mutations associated with AOI/III and LS also cause a similar discontinuity of FLNB distribution within transfected cells, but the proportion of FLNB-specific signal associated with the foci is progressively reduced, correlating with both the reduction in severity of the associated disease phenotypes albeit still with an elevated avidity for actin [Sawyer et al., 2009]. Both p.Tyr148Arg and p.Met202Val have increased avidity for F-actin [Sawyer et al., 2009] as do p.Glu254Lys in FLNA which is homologous with p.Glu227Lys in FLNB [Clark et al., 2009].

These results demonstrate marked similarities to experiments with isolated CH1 and CH2 subdomains from α-actinin-1 and filamin A that determined that a single CH1 subdomain from either molecule was necessary and sufficient for actin binding in vitro and in vivo [Lorenzi and Gimona, 2008] and that the absence of a matched CH2 subdomain adjacent to a CH1 subdomain was associated with reduced actin-filament turnover and aberrant bundling of actin fibrils. Therefore our data are consistent with a proposed model of CH1 acting as the primary F-actin-binding site and CH2 having a modulatory function.

Additionally, the data presented here also suggest that the aberrant filamin-actin binding imposed by LS-AO-BD mutations has an effect on actin cytoskeletal architecture. Similar actin focal accumulations have recently been demonstrated using a similar transient transfection approach for a gain-of-function mutation in the CH2 domain of *FLNC* [Duff et al., 2011], suggesting that the pathogenesis of this condition, a myopathy, is similar to that operating to cause the FLNA- and FLNB-related disorders. Outside the filamin gene family, a similar mechanism has been invoked for gain-of-function mutations in another actin-binding protein, α-actinin-4, which have also been demonstrated to increase F-actin binding [Weins et al., 2007].

The appearance of focal accumulations is also seen with a mutation outside the ABD in repeat 6 (p.Gly751Arg). It has been postulated that the immunoglobulin-like repeats between CH2 and the first hinge region (repeats 1 to 15) align with actin filaments and contribute significantly to actin binding [Nakamura et al., 2007]. It is therefore plausible that this mutation also increases F-actin binding in vivo.

Sections of epiphyseal growth plates from AOI/III patients contain regions of acellularity in the proliferating zone, with occasional multinucleated giant cells in the reserve zone [Sillence et al., 1982], but no observation of focal protein accumulations as have been demonstrated here employing overexpression of EGFP-labeled gene constructs. Although focused reexamination of growth plate tissue from individuals with LS-AO-BD disorders would be useful in the light of our new results, it is unlikely that anomalies like this will be identified since examination of muscle from an individual with an analogous *FLNC* mutation did not demonstrate the focal accumulations seen in transient transfection experiments similar to those performed here [Duff et al., 2011]. It is most likely that the filamin-actin foci noted here are visible because of overexpression in the transfection system employed, and may therefore not be causative of disease. Despite this, we propose that they are still reflective of a biophysical alteration in the properties of filamin that result in a maldistribution of the protein intracellularly.

In contrast to the results obtained for mutations relating directly to filamin-actin interactions, the two mutations associated with AOI/III in repeats 14 and 15 did not result in the appearance of actin-filamin containing focal accumulations. Like CH2, the repeat 14 and 15 region is a second region within which substitutions that lead to AOI/III and LS phenotypes are clustered (Fig. 1) and lies directly adjacent to hinge 1, a structure that confers flexibility to FLNB and is central to its mechanosensory properties [Gardel et al., 2006]. Deletion of hinge 1 in FLNA and FLNB has demonstrated that it is this structure that confers the nonlinear viscoelastic properties that are critical to cellular mechanoprotection conferred by filamin [Gardel et al., 2006]. Although data are lacking to directly implicate the repeat 14 and 15 mutations described here with hinge 1 function, their identical phenotypic consequences compared to ABD mutations that alter filamin transitioning within the cell through alterations in filamin-actin avidity suggest a shared impact on the cellular response to shear forces.

How this maldistribution of FLNB leads to the pathogenesis of *FLNB*-related filaminopathies is uncertain. Clearly, mutations affecting actin avidity and those around hinge 1 lead to final common phenotype that results in diminished ossification and joint dislocations. Although the mechanosensory properties of FLNB are dependent on both of these functions of the molecule, there is little understanding of how mechanotransduction influences morphogenesis in these tissues. Certainly, the position of these foci would argue against dysregulation of second messenger signaling from the cortical cytoskeleton and analogous mutations in *FLNA* do not demonstrate an abnormal migratory or cell adhesion phenotype [Clark et al., 2009]. FLNA has been proposed as an important interface between extracellular matrix (ECM) and cytoskeletal actin, acting via C-terminal associations with β-integrins [Kiema et al., 2006a; Lad et al., 2007a]. FLNB may play a similar but more specialized role in the chondrocyte, a cell type embedded within a dense ECM. Filamins confer stress-strain characteristics to actin gels in vitro similar to those observed for intact cells [Gardel et al., 2006] and furthermore extrinsic shear force, transduced via integrins, triggers filamin to change its preferred C-terminal interaction partners [Ehrlicher et al., 2011]. Increases in actin affinity, and changes to hinge flexibility, may therefore alter the gain of signals generated through integrin-filamin interaction that in turn may influence growth plate chondrocytes and osteoblasts. A critical test of this hypothesis would be the influence of hinge region mutations on FLNB flexibility, a possibility that should be addressed in future experiments.

Acknowledgments

The authors thank participating individuals and their families. SR is supported by Heath Research Council of New Zealand and Curekids, New Zealand.

References

Bicknell LS, Farrington-Rock C, Shafeghati Y, Rump P, Alanay Y, Alembik Y, Al-Madani N, Firth H, Karimi-Nejad MH, Kim CA, Leask K, Maisenbacher M, Moran E, Pappas JG, Prontera P, de Ravel T, Fryns JP, Sweeney E, Fryer A, Unger S, Wilson LC, Lachman RS, Rimoin DL, Cohn DH, Krakow D, Robertson SP. 2007. A molecular and clinical study of Larsen syndrome caused by mutations in FLNB. J Med Genet 44:89–98.

Bicknell LS, Morgan T, Bonafe L, Wessels MW, Bialer MG, Willems PJ, Cohn DH, Krakow D, Robertson SP. 2005. Mutations in FLNB cause boomerang dysplasia. J Med Genet 42:43–46.

Clark AR, Sawyer GM, Robertson SP, Sutherland-Smith AJ. 2009. Skeletal dysplasias due to filamin A mutations result from a gain-of-function mechanism distinct from allelic neurological disorders. Hum Mol Genet 18:4791–4800.

Cunningham CC, Gorlin JB, Kwiatkowski DJ, Hartwig JH, Janmey PA, Byers HR, Stossel TP. 1992. Actin-binding protein requirement for cortical stability and efficient locomotion. Science 255:325–327.

Duff RM, Tay V, Hackman P, Ravenscroft G, McLean C, Kennedy P, Steinbach A, Schöffler W, van der Ven PF, Fürst DO, Song J, Djinović-Carugo K, Penttilä S, Raheem O, Reardon K, Malandrini A, Gambelli S, Villanova M, Nowak KJ, Williams DR, Landers JE, Brown RH Jr, Udd B, Laing NG. 2011. Mutations in the N-terminal actin-binding domain of filamin C cause a distal myopathy. Am J Hum Genet 88:729–740.

Ehrlicher AJ, Nakamura F, Hartwig JH, Weitz DA, Stossel TP. 2011. Mechanical strain in actin networks regulates FilGAP and integrin binding to filamin A. Nature 478:260–263.

Farrington-Rock C, Firestein MH, Bicknell LS, Superti-Furga A, Bacino CA, Cormier-Daire V, Le Merrer M, Baumann C, Roume J, Rump P, Verheij JB, Sweeney E, Rimoin DL, Lachman RS, Robertson SP, Cohn DH, Krakow D. 2006. Mutations in two regions of FLNB result in atelosteogenesis I and III. Hum Mutat 27:705–710.

Farrington-Rock C, Kirilova V, Dillard-Telm L, Borowsky AD, Chalk S, Rock MJ, Cohn DH, Krakow D. 2008. Disruption of the *Flnb* gene in mice phenocopies the human disease spondylocarpotarsal synostosis syndrome. Hum Mol Genet 17:631–641.

Gardel ML, Nakamura F, Hartwig JH, Crocker JC, Stossel TP, Weitz DA. 2006. Prestressed F-actin networks cross-linked by hinged filamins replicate mechanical properties of cells. Proc Natl Acad Sci USA 103:1762–1767.

Gay O, Gilquin B, Nakamura F, Jenkins ZA, McCartney R, Krakow D, Deshiere A, Assard N, Hartwig JH, Robertson SP, Baudier J. 2011. RefilinB (FAM101B) targets filamin A to organize perinuclear actin networks and regulates nuclear shape. Proc Natl Acad Sci USA 108:11464–11469.

Hartwig JH, Stossel TP. 1975. Isolation and properties of actin, myosin, and a new actinbinding protein in rabbit alveolar macrophages. J Biol Chem 250:5696–5705.

Kiema T, Lad Y, Jiang P, Oxley CL, Baldassarre M, Wegener KL, Campbell ID, Ylanne J, Calderwood DA. 2006a. The molecular basis of filamin binding to integrins and competition with talin. Mol Cell 21:337–347.

Kiema T, Lad Y, Jiang P, Oxley CL, Baldassarre M, Wegener KL, Campbell ID, Ylanne J, Calderwood DA. 2006b. The molecular basis of filamin binding to integrins and competition with talin. Mol Cell 21:337–347.

Krakow D, Robertson SP, King LM, Morgan T, Sebald ET, Bertolotto C, Wachsmann-Hogiu S, Acuna D, Shapiro SS, Takafuta T, Aftimos S, Kim CA, Firth H, Steiner CE, Cormier-Daire V, Superti-Furga A, Bonafe L, Graham JM Jr, Grix A, Bacino CA, Allanson J, Bialer MG, Lachman RS, Rimoin DL, Cohn DH. 2004. Mutations in the gene encoding filamin B disrupt vertebral segmentation, joint formation and skeletogenesis. Nat Genet 36:405–410.

Lad Y, Kiema T, Jiang P, Pentikainen OT, Coles CH, Campbell ID, Calderwood DA, Ylanne J. 2007. Structure of three tandem filamin domains reveals auto-inhibition of ligand binding. EMBO J 26:3993–4004.

Lorenzi M, Gimona M. 2008. Synthetic actin-binding domains reveal compositional constraints for function. Int J Biochem Cell B 40:1806–1816.

Lu J, Lian G, Lenkinski R, De Grand A, Vaid RR, Bryce T, Stasenko M, Boskey A, Walsh C, Sheen V. 2007. Filamin B mutations cause chondrocyte defects in skeletal development. Hum Mol Genet 16:1661–1675.

Mammoto T, Ingber DE. 2010. Mechanical control of tissue and organ development. Development 137:1407–1420.

Nakamura F, Hartwig JH, Stossel TP, Szymanski PT. 2005. Ca2+ and calmodulin regulate the binding of filamin A to actin filaments. J Biol Chem 280:32426–32433.

Nakamura F, Osborn TM, Hartemink CA, Hartwig JH, Stossel TP. 2007. Structural basis of filamin A functions. J Cell Biol 179:1011–1025.

Nakamura F, Stossel TP, Hartwig JH. 2011. The filamins: organizers of cell structure and function. Cell Adhes Migration 5:160–169.

Niederman R, Amrein PC, Hartwig J. 1983. Three-dimensional structure of actin filaments and of an actin gel made with actin-binding protein. J Cell Biol 96:1400–1413.

Robertson SP. 2005. Filamin A: phenotypic diversity. Curr Opin Genet Dev 15:301–307.

Robertson SP, Twigg SR, Sutherland-Smith AJ, Biancalana V, Gorlin RJ, Horn D, Kenwrick SJ, Kim CA, Morava E, Newbury-Ecob R, Orstavik KH, Quarrell OW, Schwartz CE, Shears DJ, Suri M, Kendrick-Jones J, Wilkie AO. 2003. Localized mutations in the gene encoding the cytoskeletal protein filamin A cause diverse malformations in humans. Nat Genet 33:487–491.

Sawyer GM, Clark AR, Robertson SP, Sutherland-Smith AJ. 2009. Disease-associated substitutions in the filamin B actin binding domain confer enhanced actin binding affinity in the absence of major structural disturbance: insights from the crystal structures of filamin B actin binding domains. J Mol Biol 390:1030–1047.

Sheen VL, Feng Y, Graham D, Takafuta T, Shapiro SS, Walsh CA. 2002. Filamin A and Filamin B are co-expressed within neurons during periods of neuronal migration and can physically interact. Hum Mol Genet 11:2845–2854.

Sillence DO, Lachman RS, Jenkins T, Riccardi VM, Rimoin DL. 1982. Spondylohumerofemoral hypoplasia (giant cell chondrodysplasia): a neonatally lethal short-limbed skeletal displasia. Am J Med Genet 13:7–14.

van der Flier A, Kuikman I, Kramer D, Geerts D, Kreft M, Takafuta T, Shapiro SS, Sonnenberg A. 2002. Different splice variants of filamin-B affect myogenesis, subcellular distribution, and determine binding to integrin [beta] subunits. J Cell Biol 156:361–376.

Weins A, Schlondorff JS, Nakamura F, Denker BM, Hartwig JH, Stossel TP, Pollak MR. 2007. Disease-associated mutant alpha-actinin-4 reveals a mechanism for regulating its F-actin-binding affinity. Proc Natl Acad Sci USA 104:16080–16085.

Zheng L, Baek HJ, Karsenty G, Justice MJ. 2007. Filamin B represses chondrocyte hypertrophy in a Runx2/Smad3-dependent manner. J Cell Biol 178:121–128.

Zhou X, Tian F, Sandzén J, Cao R, Flaberg E, Szekely L, Cao Y, Ohlsson C, Bergo MO, Borén J, Akyürek LM. 2007. Filamin B deficiency in mice results in skeletal malformations and impaired microvascular development. Proc Natl Acad Sci USA 104:3919–3924.

Novel Insights from Clinical Practice

Fetal Diagnosis and Therapy

Fetal Diagn Ther
DOI: 10.1159/000335687

Received: July 13, 2011
Accepted after revision: December 7, 2011
Published online: February 18, 2012

A Case of Boomerang Dysplasia with a Novel Causative Mutation in Filamin B: Identification of Typical Imaging Findings on Ultrasonography and 3D-CT Imaging

Seiji Tsutsumi[a] Ayako Maekawa[a] Miyuki Obata[a] Timothy Morgan[b]
Stephen P. Robertson[b] Hirohisa Kurachi[a]

[a]Department of Obstetrics and Gynecology, Yamagata University Faculty of Medicine, Yamagata, Japan;
[b]Department of Paediatrics and Child Health, Dunedin School of Medicine, University of Otago, Dunedin, New Zealand

Established Facts

- Boomerang dysplasia is a rare lethal osteochondrodysplasia characterized by disorganized mineralization of the skeleton, leading to complete nonossification of some limb bones and vertebral elements and a boomerang-like aspect to some of the long tubular bones.

Novel Insights

- Demonstration of the characteristic bent bone morphology in the limbs by 3D-CT adds diagnostic certainty and facilitates prognostication and genetic counseling for parents.
- The mutation observed in this patient, c.605T>C, is the third causative mutation described in this disorder and, like the other two mutations, leads to substitution of an amino acid residue in the actin-binding domain of filamin B.

Key Words
Boomerang dysplasia · Fetal imaging · Filamin B

Abstract
Boomerang dysplasia is a rare lethal osteochondrodysplasia characterized by disorganized mineralization of the skeleton, leading to complete nonossification of some limb bones and vertebral elements, and a boomerang-like aspect to some of the long tubular bones. Like many short-limbed skeletal dysplasias with accompanying thoracic hypoplasia, the potential lethality of the phenotype can be difficult to ascertain prenatally. We report a case of boomerang dysplasia prenatally diagnosed by use of ultrasonography and 3D-CT imaging, and identified a novel mutation in the gene encoding the cytoskeletal protein filamin B *(FLNB)* postmortem. Findings that aided the radiological diagnosis of this condition in utero included absent ossification of two out of three long bones in each limb and elements of the vertebrae and a boomerang-like shape to the ulnae. The identified mutation is the third described for this disorder and is predicted to lead to amino acid substitution in the actin-binding domain of the filamin B molecule.

KARGER
Fax +41 61 306 12 34
E-Mail karger@karger.ch
www.karger.com

1015–3837/12/0000–0000$38.00/0

Accessible online at:
www.karger.com/fdt

Seiji Tsutsumi
Department of Obstetrics and Gynecology
Yamagata University Faculty of Medicine
2-2-2 Iida-Nishi, Yamagata 990-9585 (Japan)
Tel. +81 23 628 5393, E-Mail stsutsumi@med.id.yamagata-u.ac.jp

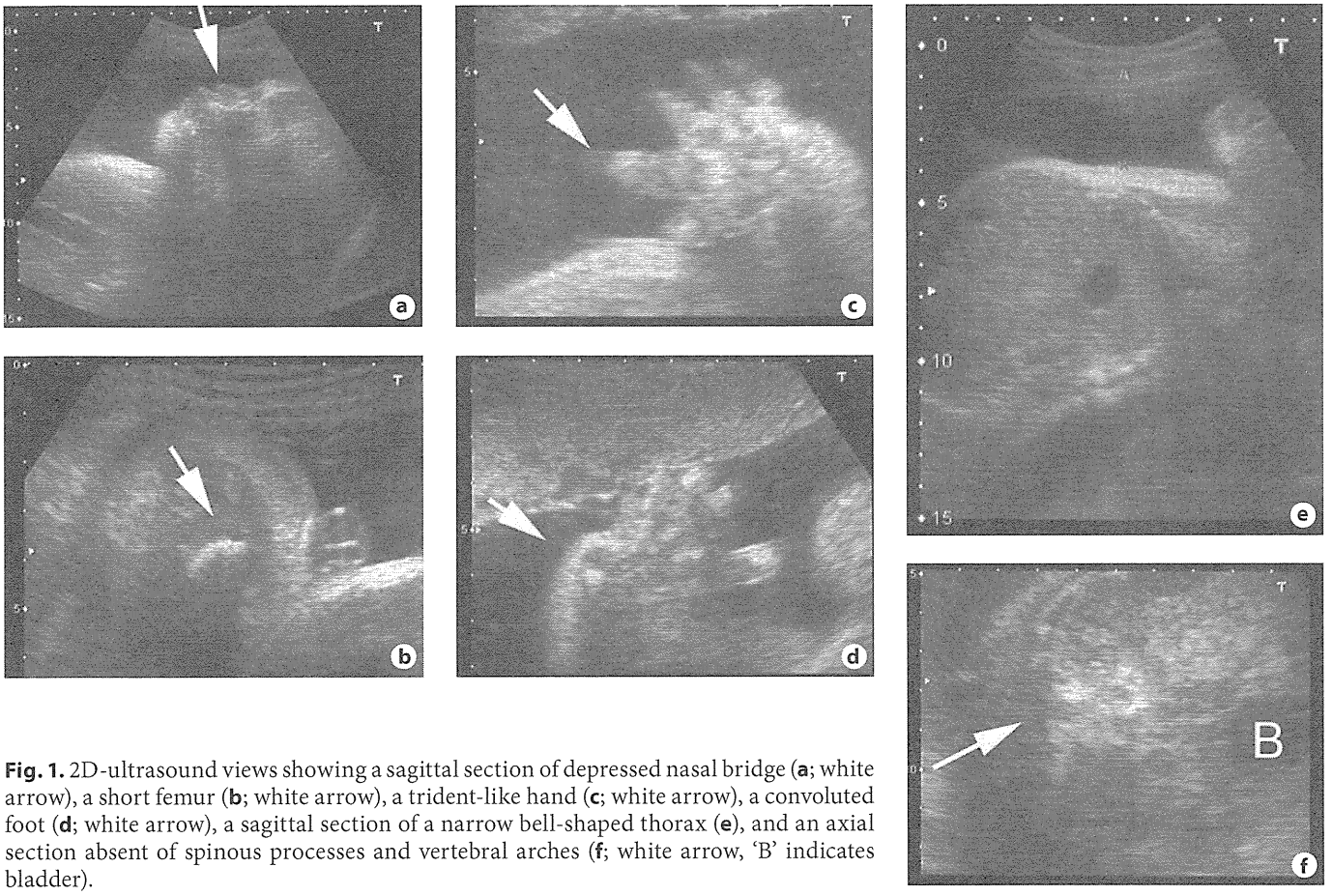

Fig. 1. 2D-ultrasound views showing a sagittal section of depressed nasal bridge (**a**; white arrow), a short femur (**b**; white arrow), a trident-like hand (**c**; white arrow), a convoluted foot (**d**; white arrow), a sagittal section of a narrow bell-shaped thorax (**e**), and an axial section absent of spinous processes and vertebral arches (**f**; white arrow, 'B' indicates bladder).

Clinical Report

This was the second pregnancy of unrelated healthy parents. The family history is noncontributory. At the time of conception the mother was 30 years old and the father 29. Routine ultrasound investigation in the 33rd week of gestation revealed severe fetal malformations, leading to referral to our hospital for prenatal diagnosis. Sonographic evaluation showed a fetus with severe micromelia. At the 33rd week of gestation, the fetal biparietal diameter was 84.8 mm (–0.3 SD), fetal trunk area was 5,808 mm^2 (–1.0 SD) and femur length was 18.2 mm (–14.8 SD). Only one of the three tubular bones was present in each limb, and the elbows and knees were indiscernible. The hands were trident and ossifications of the metacarpal bones were diminished. The bridge of the nose was flattened. The thorax was hypoplastic and had a bell-shaped appearance. The spinous processes and vertebral arches were not ossified (fig. 1). 3D-CT imaging showed the boomerang-like-shaped ulna, and the segment-shaped femur (fig. 2). In view of the typical skeletal abnormalities, including micromelia, and the absence of ossification of some but not all of the long tubular bones, the tentative diagnosis of boomerang dysplasia was made. After genetic counseling, the parents preferred not to resuscitate postpartum in view of the severity of the phenotype.

The fetus was born in the 38th week of gestation, and soon died from respiratory insufficiency. The bridge of the nose was defective (fig. 3) and a cleft palate was recognized. X-ray imaging confirmed the findings as demonstrated on the prenatal 3D-CT. Mutation analysis of the filamin B *(FLNB)* gene was undertaken on DNA extracted from umbilical cord blood after informed consent was obtained from the parents. All exons and exon-intron boundaries of *FLNB* were amplified using polymerase chain reaction as described previously [1], and amplified DNA was subjected to denaturing high-performance liquid chromatography with amplicons exhibiting anomalous waveforms subsequently sequenced on an ABI3100 sequencer. A novel mutation, c.605T>C, in exon 3 was identified, which is predicted to lead to the substitution of p.Met202Thr of the FLNB protein. This substitution occurs in the calponin homology 2 region of the actin-binding domain of FLNB.

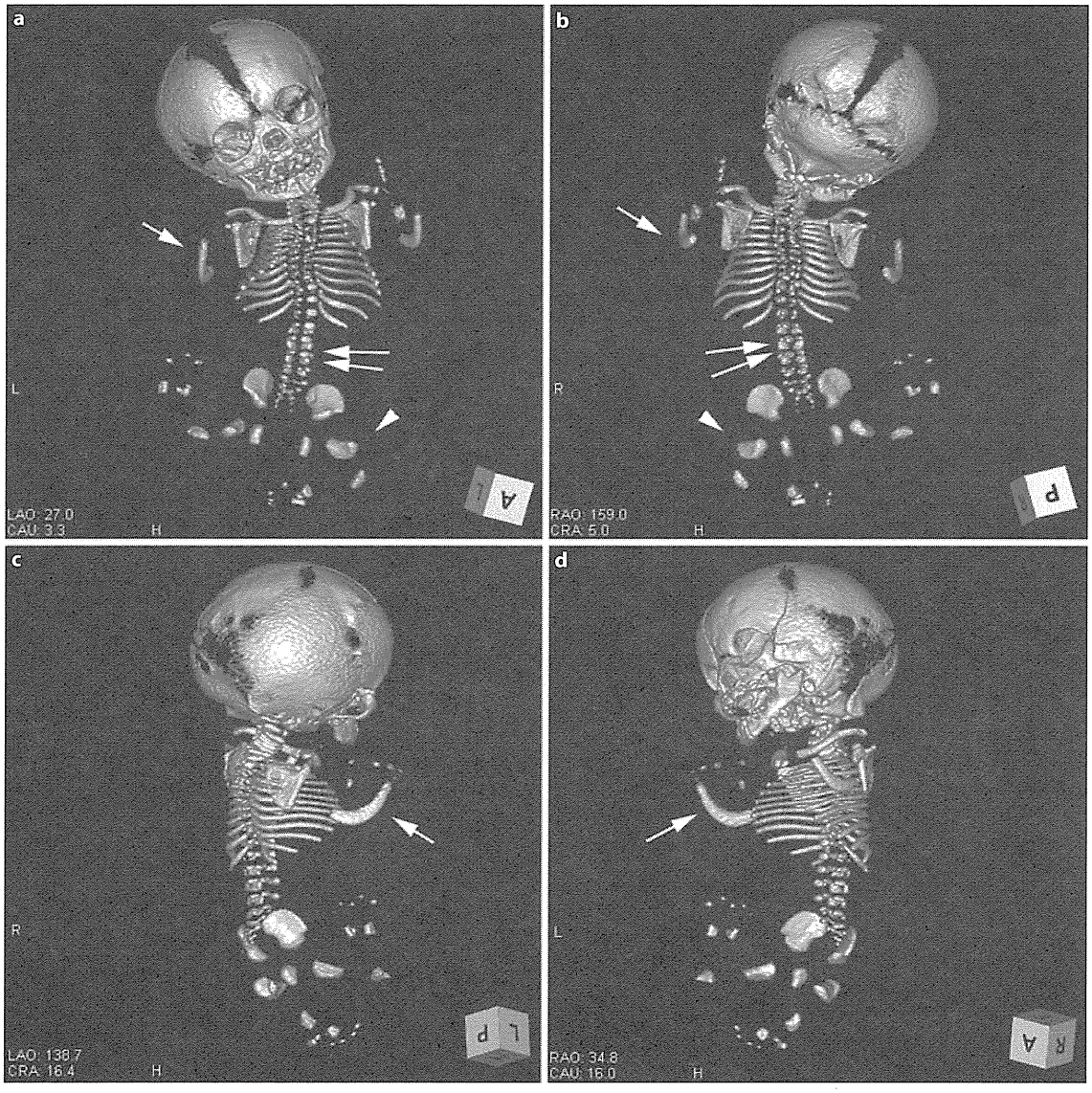

Fig. 2. 3D-CT views showing the boomerang-like shaped ulna (white arrow), the segment shaped femur (white arrow head) and zipper-like shaped spine (double arrows). The humerus and radius were absent: front view (**a**), rear view (**b**), right side view (**c**) and left side view (**d**).

Discussion

Boomerang dysplasia is a rare osteochondrodysplasia characterized by a boomerang-like aspect of the long tubular bones [2, 3]. It belongs to a family of skeletal dysplasias of varying severity, all caused by mutations in the same gene, *FLNB* [4, 5]. These related conditions in order of diminishing severity include atelosteogenesis type I and III [4] and Larsen syndrome [6]. Boomerang dysplasia is difficult to diagnose prenatally. All cases of this condition described in the literature thus far have been characterized by lethality, although instances of the phenotypically similar allelic condition, atelosteogenesis III, have been reported in conjunction with survivorship [7]. In this report we show that helical 3D-CT is a useful adjunct to obtain specific images of the skeletal abnormalities manifest in this condition.